Library
U. S. Naval Postgraduate School
Monterey, California

AN INVESTIGATION OF PARAMETERS EFFECTING THE VAPORIZATION OF FUEL UNDER CONDITIONS ENCOUNTERED IN A TURBO-JET COMBUSTION CHAMBER

A Thesis Submitted to the
Faculty of the Graduate School of the
University of Minnesota

By

Rudolph H. Koch
LCDR., U.S. Navy

In Partial Fulfillment of the Requirements
for the Degree of
Master of Science in Aeronautical Engineering

June, 1956

Thesis
K92

ACKNOWLEDGEMENTS

I wish to express my sincere appreciation to Professor Thomas E. Murphy for his guidance, encouragement and academic assistance; to Lt. Harold L. Seligmiller, USN for his advice and assistance during this project; and to Mr. William J. Alden for his cheerful advice and assistance during the modification of the equipment.

This project was sponsored by the U.S. Navy under the supervision of the U.S. Naval Postgraduate School, Monterey, California.

33165

T A B L E OF C O N T E N T S

SUMMARY

The effect of inlet air conditions on the vaporization of a benzol spray in an air stream was investigated. The fuel was injected in the direction of the air flow. The inlet air conditions were varied over the following ranges: temperature, 170 to 320° F.; velocity, 50 to 80 ft/sec.; pressure, 22.5 to 28 inches of mercury, absolute. In addition with the air conditions held constant the fuel-air ratio was varied from 0.01765 to 0.0282.

The following was determined for the conditions and ranges investigated: an increase of pressure and increase of velocity will decrease the fraction of fuel vaporized; an increase of temperature will increase the fraction of fuel vaporized; and increasing fuel-air ratio will first decrease, then increase the fraction of fuel vaporized.

As a result of this investigation is was determined that the basic equipment in its present configuration is not satisfactory for the quantitative investigation of fuel sprays

This project was sponsored by the U.S. Navy and conducted under the auspices of the Mechanical and Aeronautical Engineering Departments of the University of Minnesota

SYMBOLS

The following symbols are used in this report:

A	area	$ft.^2$
C	circumference	ft.
c	specific heat	BTU/lb.-^oF
c_p	specific heat at constant pressure	BTU/lb.-^oF
D	diameter	ft.
F	fuel-air ratio	----
H_v	heat of vaporization	BTU/lb.
h	surface film heat transfer coefficient	BTU/ft^2-hr-^oF
k	thermal conductivity	BTU/ft^2-hr-^oF/ft.
L	length of immersion	ft.
m	mass flow rate	lb/sec.
P	pressure	lb/ft^2
$(P_{dy})_{al}$	pressure	in. alcohol inclined at 30°.
$(P_{ts})_h$	pressure	in. mercury, absolute.
q	heat	BTU
T	temperature	^oR
t	temperature	^oF
ΔT	temperature difference between "wet" and "dry" readings	^oF

X	fraction fuel vaporized	----
x	streamwise distance in test section	in.
y	vertical distance	in.
Y	height of tunnel at any section	in.
σ	Stefan-Botlzmann constant	$BTU/hr\text{-}ft^2\text{-}T^4$
ϵ	emissivity	----
ρ	density	lb/ft^3
μ	absolute viscosity	lb/hr-ft

Subscripts:

a	air	t	thermocouple
ab	ambient	ts	test section
al	alcohol	w	water
c	conduction	I	initial
cv	convection	II	final
dy	dynamic	()'	shield
e	end		
f	fuel		
g	gage		
h	mercury		
m	wall		
n	any position n		
o	orfice		
r	radiation		
s	shield		

INTRODUCTION

The vaporization of a liquid fuel in the pre-combustion zone of the turbo-jet combustion chamber is an important step in the combustion process. The vaporization process is effected by such parameters as:

a) the air stream temperature, velocity and pressure.

b) the fuel-air ratio.

c) the spray characteristics such as degree of atomization, drop size, drop size distribution and drop velocity.

d) the fuel characteristics.

A knowledge of the effect of these parameters is important in the rational design of the combustion chamber. An accurate prediction of the fraction vaporized, as a function of distance from the injector, along with the fuel distribution in the spray, would determine the local fuel-air ratio, thus determining the location of the point at which ignition could take place.

The various investigators have worked on the problems of fuel spray vaporization. The early investigations date back to the 1930's, and deal with the problems of spray vaporization as applied to the compression ignition internal combustion engine.

The more recent investigations are of two general classes, those approaching the problem from a single drop analysis, and those investigating the vaporization of the spray as a whole.

Some of the single drop investigations are reported in Ref. 1 through Ref. 4.

The vaporization rate and the heat transfer coefficients for pure liquid drops were determined in the investigation reported in Ref. 1. This investigation resulted in a semi-emperical equation, relating the vaporization rate, to the temperature difference between the air and the surface temperature of the vaporizing drop. It was also shown that the temperature of the fuel when injected had little effect on the vaporization rate.

The effect of static pressure on the vaporization rate of single drops was determined by the investigation of Ref. 2. The static pressure effected the vaporization rate only to the extent that it influenced the surface temperature of the vaporizing drop. The semi-emperical equation determined in the investigation of Ref. 2, is very similar to the equation reported in Ref. 1.

The vaporization of the fuel drops during the time they are heating or cooling to their wet bulb temperature was theoretically investigated in Ref. 3. The investigation has shown this period to be important and to be of such extent that drops may reach the combustion zone while still in the unsteady state.

The theoretical results reported in Ref. 3 are experimentally verified in the investigation as reported by Ref. 4, and shows that the unsteady state during which the drop is heating or cooling is important, and may be a major portion of the vaporization time.

The investigations of Ref. 1 through Ref. 4, provide considerable insight into the basic processes controlling and effecting vaporization, but provide little information as to the effect of various parameters applied directly to the fuel sprays. The investigations reported in Ref. 5 through Ref. 7 consider the entire spray. The results are reported as fraction of fuel vaporized as a function of distance from the injector, correlating air stream and fuel conditions in various manners.

The vaporization of JP-5 fuel in an air stream was investigated as reported in Ref. 5. The fraction evaporated was related by a semi-emperical equation; to the distance from the injector, the difference between the wet bulb temperature of the drops and the air, the fuel injection velocity, and the air stream velocity. The effect of pressure is reflected in the difference between the wet bulb temperature and the air temperature. The equation determined for the range of variables investigated is:

$$N = 7.4\, L^{0.33}\, \Delta T^{0.28} \left[\frac{U_a + U_f}{100 + U_a}\right]^2$$

where N is the percentage of JP-5 fuel evaporated, L is the distance downstream from the injector (in.),

ΔT is the difference between the air and the wet-bulb temperature (^{o}F), U_a is the air velocity (ft/sec), and U_f is the fuel-injection velocity (ft/sec).

The vaporization of iso-octane sprays is reported in Ref. 6 and Ref. 7.

The vaporization of an iso-octane spray injected contrastream through a simple orfice into a high velocity air stream is reported in Ref. 6. This investigator was able to correlate, through a semi-emperical equation; the effect of air temperature, air velocity, air pressure, fuel injection pressure and distance from the injector. The outstanding result was that the large driving force of air temperature was clearly shown. The equation determined for the range of variables investigated is:

$$\frac{N}{100-N} = 9.35 \left[\frac{Ta}{1000}\right]^{4.4} \left[\frac{Va}{100}\right]^{0.8} P_a^{-1.2} P_f^{0.42} L^{0.84}$$

where N is the percentage of iso-octane evaporated, T_a is the air temperature (^{o}R), V_a is the air velocity (ft/sec), p_a is the air pressure (in.Hg.Abs.), p_f is the fuel injection pressure ($\#/in^2$), and L is the distance downstream from the injector (in.)

The investigation of Ref. 7 determined drop size distribution and drop velocity in the spray by photographic techniques and correlated this with some of the previous single drop results. The investigators were also able to verify the results reported by Ref. 6.

The present investigation deals with the vaporization of benzol injected in the direction of the air stream from a high velocity nozzle, and the effect on vaporization by:

a) air stream temperature

b) air stream pressure

c) air stream velocity

d) fuel-air ratio

The mixture temperature was measured at two downstream stations, $9\frac{1}{2}$ and $16\frac{1}{4}$ inches from the nozzle. The inlet air conditions were varied over the following ranges: air temperature, 170 to 320°F; air velocity, 50 to 80 ft/sec; and air pressure, 22.5 to 28 inches of mercury, absolute. The fuel-air ratio was varied from 0.01765 to 0.0282 corresponding to a fuel pressure variation of 75 to 175 lb/in^2. The vaporization was found to be a function of temperature, pressure, velocity and fuel-air ratio.

APPARATUS

Basic Equipment

The test equipment used in this project is shown in the schematic drawing of Fig. 1, and in the photographs of Fig. 2 through Fig. 7. The basic equipment is a small open circuit wind tunnel with provisions to spray fuel into the 4 x 4 x 20 inch test section under varying air stream conditions. Incorporated in the test section is instrumentation to measure the condition of the fuel-air mixture as it proceeds down the test section. Measuring stations and numbering are shown in Fig. 4 and Fig. 8.

The basic test equipment, described in detail in Ref. 8 and Ref. 9, required extensive modification to enable independent variation of the parameters; static pressure, velocity and temperature. The maximum ranges obtainable were approximately as follows:

Static pressure- 0.5 to 10.0 in. Hg., vacuum

Velocity- 50 to 250 ft/sec

Temperature- Ambient to 400° F.

Fuel flow- 3.5 to 7.5 gal/hr

The usable range is considerably smaller since the extremes of each parameter could not be attained at the same time nor could the extremes be reached in all cases when one or more parameters was held constant.

The air in the tunnel was heated by 12 Chromolox, 230 volt, 2450 watt finstrip electric heaters. The switches

and fuses were so arranged that any combination of heaters ON could be obtained. One heater circuit contained a rheostat in order to give close control of air temperature. The heater control panel is shown in Fig. 3. The physical location of the heaters in the tunnel is shown in Fig. 1, with the relative arrangement of the heaters for two configurations is shown in Fig. 9.

The test section temperature profiles are very poor. Considerable time and effort were expended in attempts to improve the profiles but to no avail.

The air pump for the wind tunnel is a centrifugal compressor driven by an air cooled Lycoming tank engine. The compressor and engine shown in Fig. 6, are located in the same room and in close proximinity to the tunnel. This arrangement made operation at high vacuum in the tunnel difficult. To operate at a high vacuum the engine and compressor speed had to be near the maximum allowable, resulting in a noise level that was untenable for the time required to take extensive data.

Instrumentation

The primary instrumentation required was for the measurement of the air temperature, pressures and velocity as it entered the test section and the measurement of the fuel-air mixture temperature at two stations in the test section. Other measurements to be made were air inlet temperature to the tunnel, compressor air inlet temperature, fuel bath temperature, fuel probe coolant water exit temperature, fuel flow, fuel pressure, and atmospheric pressure. A general view of the instrumentation is shown in Fig. 5.

All temperatures were measured by the use of iron-constantan thermocouples wired to a switch board and read by a direct indicating Leeds and Northrop potentiometer.

The velocity, or dynamic pressure was measured by use of a U-tube alcohol manometer inclined 30° to the horizontal. So the dynamic pressure could be read directly, one side of the tube was connected to the total pressure probe and the other side connected to a static pressure orfice.

Static pressure measurement in the test section was made by use of a mercury manometer.

The air inlet temperature was measured by a bare thermocouple located at the tunnel inlet throttle valve.

The compressor inlet temperature was measured by a bare thermocouple projecting approximately one inch into the compressor inlet pipe at a point approximately six feet from the compressor.

Fuel bath temperature was measured by a thermocouple immersed in the fuel bath.

Fuel probe coolant water exit temperature was measured as the water left the fuel probe by a thermocouple immersed in the flow.

Fuel flow was measured by a calibrated rotometer with the pressure being measured by the CO_2 pressure applied to the fuel tank.

Atmospheric pressure was measured by a conventional mercury column barometer.

The measurement of the test section temperatures required the construction of three special thermocouple probes, each of a special and different configuration. These probes are shown in Fig. 7.

The configuration (a) of Fig. 7 was used to measure the test section inlet air temperature. This configuration employed a simple cylindrical shield to reduce the radiation losses to the wind tunnel walls.

The measurement of the fuel-air mixture temperature is a difficult problem. In an attempt to arrive at a satisfactory solution, two different configurations were constructed and used during the tests. The configuration (b) of Fig. 7 consists of a sensing element shielded by a semi-circular shield, convex side into the airstream, with the element located just behind the shield. A second sensing element was fastened to the downstream side of the shield itself.

This second element should measure the shield temperature and provide a possible basis for estimating the error of the air sensing element, as well as giving the temperature of the liquid drops in the spray.

The configuration (c) of Fig. 7 employs two concentric cylinders plus a flat circular plate ahead of the cylinders to shield and keep dry the sensing element.

Fuel System

The fuel system consists of the nozzle, rotometer, tank, filter, pressure gage, method of pressuration, valves and piping.

The fuel tank is pressurized by high pressure CO_2. The fuel is filtered as it leaves the tank and passes through the calibrated rotometer to the nozzle. The rotometer has a capacity of 15 gal/hr and could be read to an accuracy of 0.1 gal/hr.

Valving and piping was provided to shut off the fuel at the rotometer and at the entrance to the probe, as well as providing means for use of water in the spray nozzle.

The nozzle of the system is of the high velocity type having a capacity of 5 gal/hr, at a pressure of 100 lb/in^2. The nozzle provides a 60^o cone of spray. The spray is essentially a hollow cone type, but may posses some solid cone spray characteristics.

EXPERIMENTAL PROCEDURE

Due to the unfavorable temperature profiles, large errors in absolute values could easily enter the investigation. To minimize the variables during the investigation, special care was taken to maintain constant as many factors as possible. Care was taken to maintain the same sequence of events during all runs. Since heater pattern had an effect on the temperature profile, the number of heater patterns used was kept at a minimum, and the same heater pattern used whenever possible.

The reference temperature was always taken at position 1, $2\frac{1}{2}$ inches up from the bottom of the test section. The reference velocity was always taken at position 2, $2\frac{1}{2}$ inches up from the bottom of the test section. The static pressure was measured at the test section entrance. The mixture temperatures were taken at positions 9 and 10, $2\frac{1}{2}$ inches up from the bottom of the test section. The level of $2\frac{1}{2}$ inches up from the bottom was chosen as the measuring level since based on preliminary runs, it was noted that the temperature read at this level was in many cases close to the average temperature obtained by graphical integration of the temperature profile.

By use of the foregoing procedure, and applying the same technique in all situations, it was hoped that the results would reflect the effect of the primary parameters to a maximum degree.

Data was collected under conditions of varying temperature, velocity, pressure and fuel-air ratio.

The procedure used during the runs in which temperature was the primary variable was as follows:

The tunnel was operated at a low speed and a low mass flow rate with the heaters ON until the temperature neared the operating temperature corresponding to the number of and pattern of heaters used. Then the static pressure and velocity was adjusted near the desired values by manipulation of the inlet air throttle, the bleed valve and compressor RPM. Since these are a function of temperature, minor adjustments were made until all factors reached the values as dictated by the equilibrum temperature corresponding to the number of heaters being used. Operating curves of dynamic pressure and fuel flow versus temperature and velocity were plotted to facilitate operation of the tunnel. The equations of these curves are developed in the Appendix.

When conditions were at equilibrum, readings of temperature at positions 1, 9, 9' and 10, velocity at position 2, and static pressure at test section entrance were taken. Fuel then was injected at a rate to give the desired fuel-air ratio. These readings were taken again when the temperatures had stabilized (approximately 1 to 2 min.), giving a "dry" and "wet" reading. The fuel was shut off, the temperature level changed and the procedure repeated until data had been collected at four different temperature levels.

During all runs in which temperature was the primary variable, four heater patterns were used:

Pattern I: heaters 2,3,7,10,11.

Pattern II: heaters 2,3,5,6,7,10,11.

Pattern III: heaters 2,3,5,6,8,9,7,10,11.

Pattern IV: heaters (all) 1 through 12.

Data was always taken in order of increasing temperature.

When the other parameters were varied the procedure was very much the same, in that, the controls were continuously adjusted until equilibrum was reached. A "dry" reading was taken, the fuel then injected at the rate dictated by the desired fuel-air ratio. When the temperatures had stabilized, the "wet" readings were taken and fuel shut off. Then the settings were readjusted to the new condition and the procedure repeated until sufficient data was obtained.

A sample data sheet with raw data from a typical run is shown as Table I.

RESULTS AND DISCUSSION

Test Section Temperature Gradient

The heating of the air and temperature gradient in the test section have been and still are the major difficulty plaguing the basic equipment used for this project. This temperature gradient is so serious that only qualitative data could be taken. The temperature gradient occurs on a vertical surface perpendicular to the flow of air, becoming more pronounced as the temperature level in the tunnel increases, and as the mass flow rate decreases. The temperatures are nearly constant in the horizontal plane and in the direction of the air stream.

In Fig. 10, are shown temperature profiles at various positions in the test section. These profiles show a temperature variation of about 95°F. The range of temperature variation, shown by profiles in the test section for various operating conditions, was from 60°F. to 120°F. With reference to Fig. 10, it should be noted that the temperature variation at any level in the test section is relatively small, and that the profiles at the various positions have very nearly the same shape. Due to the limited access to the test section and due to the construction of the probes, it was not possible to measure the temperature closer than one-half inch to the wall. It would be expected that the air would be cooled at the walls, and this was verified by a limited number of measurements.

The curves of Fig. 11 are temperature profiles at various operating conditions, taken at position 1, the entrance to the test section. These profiles show the increase of the gradient as the temperature level in the tunnel is raised. Considerable time and effort went into attempts to determine the cause of and correction of the temperature gradient.

The first attempted solution was to insulate the outside of the tunnel between the heaters and the test section. This was an attempt to improve the temperature gradient and also to decrease the heating time required to bring the tunnel to a near equilibrum temperature. The heating time reported by previous investigators (Ref. 8 and Ref. 9) as approximately one and one-half to two hours was reduced to approximately 20 minutes as shown by Fig. 12. The insulation had no noticeable effect on the temperature profiles.

The next step involved the variation of the heater pattern, both by turning OFF or ON various heaters and by physical rearrangement. By varying the pattern of heaters turned ON, it was possible to improve the profile, but not to a satisfactory degree. The turning OFF of some of the heaters also lowered the maximum temperature obtainable. Fig. 13 shows two profiles with different heater ON configurations. The profile at the lower temperature level and small number of heaters shows a smaller gradient. In this configuration all heaters ON are at or below the center line of the tunnel. In spite of this the maximum temperature still occurs above the centerline.

The physical rearrangement of the heaters as well as the original configuration is shown in Fig. 9. The addition of the 12th heater to the tunnel raised the general temperature level in the tunnel but did little, if anything, to improve the profiles. The rearrangement of the heaters was to no avail.

In attempt to further study and determine the cause of the unsatisfactory profile in the test section, temperature profiles were taken at the exit from the heaters, near the middle of the settling chamber, and at the entrance to the contraction section going to the test section. These profiles are shown in Fig. 14. In study of these profiles, it should be noted that the maximum temperature occurs at a higher point on the profile as the air proceeds through the tunnel. Also to be noted is the cooling near the walls. These two effects would indicate that the profile is caused, in part, by the heat transfer to the walls and by the convective lifting of the air as it moves slowly through the settling chamber. The velocity in the settling chamber is of the order of 2.0 ft/sec with a test section velocity of 50 ft/sec. Other contributing causes may be uneven flow and heating as the air passes through the heater section. This uneven heating and quite possibly, uneven flow is shown by the profile as the air leaves the heater section. Cross-currents in the tunnel or lack of symmetery of the contraction section could also aggravate the situation.

Time limitations prevented further study of this problem, and possible major modification was ruled out. The presence of the gradient eliminated the possibility of obtaining good quantitative data. The tests proceeded in hopes of getting qualitative data that could be interpreted to show the effect of the parameters under study.

Mixture Temperature Thermocouples and Estimation of Thermocouple Error

The configuration (b) of Fig. 7 was designed to keep the sensing element dry and by use of the shield thermocouple, make an accurate estimate as to the radiation error of the element. The element appeared to stay dry except when the liquid concentration was very high. The thermocouple on the shield gave readings that would indicate that the shield was wetted by the liquid fuel.

The configuration (c) of Fig. 7 was designed for the same purpose. To largely eliminate radiation errors, the sensing element was surrounded by two concentric cylinders, the forward end being obstructed by a circular flat plate placed about one-eighth inch ahead of the cylinder. In this manner it was hoped the liquid drops would be eliminated from the air that would flow over the element and between the two concentric cylinders. The outside cylinder and the plate would be wet to a varying degree and be at a temperature approaching that of the liquid. The inside cylinder would be dry and at a much higher temperature, at a temperature approaching that of the mixture and the sensing element. This should make the radiation errors very small.

The temperatures measured by the two temperature probes of Fig. 7, (b) and (c), when placed at the same point in the test section under the same operating conditions, either "dry" or "wet", did not differ by a significant amount. The variation was of the order of three degrees. In spite of the close agreement of the two configurations, the true temperature of the fuel-air mixture is still not known.

The thermocouple "reads" the temperature that the sensing element itself attains. The temperature that the element attains is a function of how much heat is transferred from the fluid to the sensing element, and how much is lost by the sensing element, to its surroundings. At low velocities the largest sources of errors are due to the radiation and conduction losses. In many cases the errors due to conduction are very small, and may be neglected. This is not the case for the probes used during this project to measure the mixture temperature. It was carefully noted that for the same operating condition when taking "wet" readings, the temperature read, differed depending on whether the probe was inserted from the top or bottom of the test section. When inserted from the top the "wet" readings were about six degrees higher than when the probe was inserted from the bottom. This variation can be explained by the fact that when the probe is inserted from the top, the supporting tube is exposed to higher temperatures (due to the temperature gradient). Thus, when the fuel is injected for short periods of time less heat will flow from the junction by conduction

(may even flow toward the junction) thus giving a higher temperature reading. When inserted from the bottom, the tube is exposed to a lower temperature, and hence, when the fuel is injected more heat is lost by conduction, and therefore, a lower temperature reading.

To estimate the order of the error between the thermocouple and the true mixture temperature an attempt was made to calculate the temperature of the thermocouple sensing element of configuration (b) of Fig. 7. To do this the thermocouple and its supporting tube are considered to be fins. The supporting tube to be a fin projecting from the tunnel wall and the thermocouple sensing element to be a fin projecting from the end of the supporting tube.

The equation that applies is:

$$(t_e - t_a) = \frac{t_m - t_a}{\text{Cosh } Ml} \qquad \text{also} \quad M = \sqrt{\frac{hC}{kA}}$$

where t_e is the temperature of the free end of the fin (^oF), t_a is the temperature of the air (^oF), t_m is the temperature of the wall (^oF), l in the length of the fin (ft.), h is the surface film heat transfer coefficient ($BTU/ft^2\text{-}hr\text{-}^oF$), C is the circumference of the fin (ft.), k is the thermal conductivity of the fin ($BTU/ft^2\text{-}hr\text{-}^oF/ft$), and A is the area of the fin that conducts heat (ft^2). The equation is developed in Ref. 11 and applied in a manner very similar to the situation now under consideration, in Ref. 12. The equation is first applied to the supporting

tube to obtain the temperature of the end of the tube supporting the thermocouple junction. It is then applied to the thermocouple, the end of the supporting tube then becoming in effect the wall for the thermocouple junction.

The radiation loss can be considered by including it in the heat transfer coefficient in the term M, so that $h = h_{cv} - h_r$. The results of the calculations for typical conditions in the tunnel show an error of the order of $5\,^{o}F$. The detailed calculations and assumptions are given in the Appendix.

Air Temperature Drop Due to Fuel Vaporization

The heat required to vaporize the fuel spray in an air stream, is taken from the air stream. It is therefore possible, knowing the initial fuel temperature, the initial air temperature, the fuel-air ratio, the final fuel temperature, and the final air temperature, to calculate the fraction of fuel vaporized. The expression relating these quantities is as follows:

$$\dot{m}_a c_{p_a}(T_{a_I} - T_{a_{II}}) = \dot{m}_f X H_v + \dot{m}_f X c_{p_f}(T_{a_{II}} - T_{f_I}) + \dot{m}_f (1-X) c_{p_f}(T_{f_{II}} - T_{f_I})$$

let $F = \frac{\dot{m}_f}{\dot{m}_a}$ and $\Delta T = (T_{a_I} - T_{a_{II}})$

$$\Delta T = \frac{FXH_v}{c_{p_a} + FXc_{p_f}} + \frac{FXc_{p_f}}{c_{p_a} + FXc_{p_f}}(T_{a_I} - T_{f_I}) + \frac{F(1-X)c_{p_f}}{c_{p_a} + FXc_{p_f}}(T_{f_{II}} - T_{f_I})$$

where $\dot{m}$ and $\dot{m}_f$ are the flow rates of air and fuel respectively (lb/sec), c_{p_a} and c_{p_f} are the specific heats at constant pressure of air and fuel respectively (BTU/lb-^{o}F.),

F is the fuel-air ratio, H_v is the heat of vaporization of the fuel (BTU/lb), T_{a_I} and T_{f_I} are the temperatures of air and fuel prior to fuel injection respectively (^oR), $T_{a_{II}}$ and $T_{f_{II}}$ are the fuel and air temperature at a given time or station after fuel injection (^oR), and X is fraction of the fuel vaporized. The first term is the air temperature drop due to the vaporization of the fuel, the second term is the temperature drop due to the heating of the vaporized portion of the fuel from its initial temperature to the final air temperature, and the third term is the temperature drop due to the heating of the unvaporized portion of the fuel from its initial temperature to the fuel drop wet-bulb temperature. The maximum temperature drop would occur when the fuel has completely vaporized. The expression then becomes, since X = 1.0:

$$\Delta T = \frac{FH_v}{c_{p_a} + Fc_{p_f}} + \frac{Fc_{p_f}}{c_{p_a} + Fc_{p_f}} (T_{a_I} - T_{f_I})$$

For the fuel-air ratio 0.01925, a value frequently used during this test; an initial air temperature of 220°F., near the middle of the temperature range investigated; and using the initial fuel temperature of all the tests, ΔT for complete vaporization is approximately 20°F.

Now writing the same equation as for ΔT, but separating the fraction vaporized X, the expression becomes:

$$X = \frac{c_{p_a} \Delta T - Fc_{p_f} (T_{f_{II}} - T_{f_I})}{F\left[H_v + c_{p_f} (T_{a_{II}} - T_{f_{II}})\right]}$$

By examination of the above expression, the first term in the numerator is the heat taken from the air stream. The second term is the heat required to heat the fuel from its initial temperature to the final or wet-bulb temperature of the fuel. The difference of the two is the heat used for vaporizing the fuel and super-heating the fuel vapor to the final air temperature. The first term in the denominator is the heat of vaporization, the second term is the super-heat required. Therefore for the fuel-air ratio F, a ratio of the heat used to that required is the fraction vaporized. The final fuel temperature can be determined by the methods of Ref. 1.

Fuel-Air Distribution in the Spray

The injection of fuel into an air stream by a simple orfice, essentially from a point source, gives a bell shaped curve such as shown in Fig. 15. The spray used during this project is a hollow cone type of spray, a spray originating essentially from a ring source. It would be expected that the fuel-air distribution for this type of spray would be as indicated by the second curve in Fig. 15.

In an attempt to determine the fuel-air distribution for the spray used during this project, two vertical traverses of the spray were made, one on the centerline, and the other, one inch off the centerline. A plot of the temperature drops of the thermocouple on the shield at a station 9½ inches downstream from the nozzle is shown in Fig. 16. The magnitude of these temperature drops is an indication of the liquid fuel-air ratio in the spray. Even though the temperature drop is a function of the liquid fuel-air

ratio, there is no evident relationship to give the actual numerical value of the liquid fuel-air ratio.

Since the spray was impinging on the center portion of the test section walls it is evident that the measurements taken covered only a portion of the spray had it been allowed to take its natural shape. The experimental points taken one inch off the centerline cover an area in which the fuel does not impinge on the walls and the decrease of the fuel-air ratio outside the spray is indicated by the points near the bottom of the test section. One inch off the centerline, no measurement could be obtained closer than within one inch of the lower wall, but assuming symmetery, the dotted portion of the curve may be added. This gives a curve very similar to the assumed curve. Even though the experimental data is very rough and sparse, it appears the experimental data verifies the assumed fuel-air distribution. Visual observation of the spray verified the high liquid concentration near the edge of the spray.

Range and Collection of Data

The range over which data was collected was determined, at one limit, by the capacity of the fuel system. It was decided to maintain a constant fuel-air ratio when varying temperature, pressure and velocity. Since the maximum capacity of the fuel system was about 5.2 gal/hr., the upper limit of the mass flow was fixed by this value.

Since the minimum allowable velocity in the test section is about 50 ft/sec., to insure sufficient flow over the heaters, the lower limit of mass flow was fixed by the velocity requirement.

Since a minimum of four points in each run was desired, a point was taken at the minimum, one at the maximum, and two at approximate equal increments between the limits.

The choice of the fuel-air ratio was based on the requirement of having as high a fuel-air ratio as possible and still have a reasonable spread of the other variables. These considerations fixed the fuel-air ratio at 0.01925 for all runs, except where the fuel-air ratio was the variable. To maintain this fuel-air ratio at varying velocities, required the velocity data to be taken between 50 and 80 ft/sec. The data taken under conditions of varying pressure was taken between 28 and 22.5 inches of mercury, absolute, the lower limit being determined by the equipment and the human limitations. The data taken under varying temperature conditions was limited by the heater capacity and by the limit imposed by using a given set of heater patterns.

The procedure of measuring the mixture temperature at only one point in each of two planes perpendicular to the flow was the result of the following line of reasoning. Assuming that the fuel-air distribution curve, as shown in Fig. 15, would remain fairly constant, a point could be

selected that would give in one reading the same value that would be given by a traverse and subsequent integration of the traverse values. The large saving in running time, and saving of fuel was also an important consideration. The particular point, one half inch above the centerline, was chosen more on the basis of having the probe at a point where a near average temperature was being read, rather than from the fuel-air distribution considerations. After the completion of the tests, it was noted in Ref. 5 that the investigators used a one point measuring technique with a spray from a simple orfice. The point at which they obtained the same reading as the integrated value was one-half inch off the centerline of the spray.

Presentation of Results

The results of these tests are presented in Fig. 17 through Fig. 20 as plots of ΔT versus the variable under consideration. ΔT is the difference between the "dry" reading and the "wet" reading at a particular position, and not the difference between the "wet" reading at a position and the inlet air or reference temperature at position 1. In many cases the "dry" reading at the particular position and the reference temperature were identical. It was assumed that ΔT is some function of the amount of fuel vaporized. There is no attempt to relate ΔT to the fraction of fuel vaporized other than; the greater the ΔT, the larger the fraction of fuel vaporized.

Little significance can be attached to the magnitude of ΔT. Errors in the "wet" temperature measurements are estimated to be of the order of five degrees under typical operating conditions. This estimate evidently is too low, since the maximum temperature drop under typical operating conditions, assuming complete vaporization is about 19°F. A traverse of the spray under these same conditions revealed a minimum temperature drop of 27°F., a maximum ΔT of 48°F., with an average ΔT approximately 35°F.

Effect of Inlet Air Temperature

The effect of inlet air temperature on ΔT is to increase ΔT with higher inlet air temperatures. This is plotted in Fig. 17 for the two measuring positions; position 9, 9½ inches from the nozzle, and position 10, 16, inches from the nozzle. The ΔT at position 10, is always less than the ΔT at position 9. This is not a thermocouple peculiarity, since the two thermocouples were checked under identical conditions, and gave near identical readings. This condition may be explained in the following manner; it appears the fuel is completely vaporized at or near position 9, and as the fuel-air mixture proceeds down the test section it is heated from the test section walls, which are nearly at the "dry" temperature. This then gives the smaller ΔT as shown in Fig. 17. The general trend of the results agree with the results obtained for iso-octane and JP-5 as reported in Ref. 5 and Ref. 6.

The increase of inlet air temperature is reflected by the larger temperature difference between the air and the surface temperature of the drop. This temperature difference is a very large driving force in the vaporization process.

Masked in the ΔT obtained for varying temperatures are the effects of the change of spray characteristics. These changes are due to the changes of fuel flow and fuel pressure. With increasing air temperature, the fuel flow and fuel pressure are reduced. This will decrease the drop velocity and increase the drop size. The drop penetration will decrease due to the reduced pressure, but may increase due to the reduced air density. The decrease of drop velocity due to reduced fuel flow, will for this operating condition, increase the relative velocity of the fuel and air, and will increase the rate of vaporization. The effect of the spray characteristics will enter and be included in all cases under investigation. These effects have varying degrees of significance.

Effect of Static Pressure

The effect of test section pressure on ΔT is to increase ΔT with a decrease of static pressure. Fig. 18 gives the results at a reference temperature of 236°F., velocity of 70 ft/sec. and fuel-air ratio of 0.01925. Once again the general trend of these results agree with those reported for iso-octane and JP-5 in Ref. 2, Ref. 5 and Ref. 6.

The reduction of ΔT with increased pressure is the result of a number of factors. As pressure is increased, the difference between the air temperature and the surface temperature of the fuel drop is decreased, thus reducing vaporization. As the pressure is increased, the relative velocity of the fuel and air is reduced, also reducing vaporization. The residence time may or may not undergo a net change as a result of increased fuel velocity and reduction of penetration due to increased air density.

Effect of Fuel-Air Ratio

The effect of fuel-air ratio on ΔT is shown in Fig. 19. The value of ΔT passes through a minimum at a fuel-air ratio of about 0.0235. The minimum value of ΔT occurs at a fuel-air ratio that corresponds to a velocity of fuel leaving the nozzle that is nearly equal to the air stream velocity. Since the relative velocity between the fuel and air is an important factor in the rate of vaporization, the lack of this relative velocity may account for the minimum ΔT at this fuel-air ratio.

When the fuel air ratios are richer than the fuel-air ratio at minimum ΔT, the ΔT measured at positions 9 and 10 are identical. Due to the larger mass flow rates of fuel, the identity of the two readings may be the result of the continued vaporization taking place further downstream. The heating from the walls takes place for a shorter period of time, has less effect, with a larger

resulting temperature drop at position 10. The increased penetration at high fuel flows may also cause the vaporization to take place further downstream. The residence time increases as the fuel velocity is decreased, and would tend to increase the fraction vaporized at the lower fuel-air ratios.

Effect of Air Stream Velocity

The effect of air stream velocity on ΔT is to decrease ΔT with increased velocity. This is shown in Fig. 20. As the air velocity is increased, the fuel flow and hence the fuel velocity is increased but the relative velocity between the air stream and the fuel varies little. The penetration of the drops will increase at the higher fuel and air velocities. These factors both tend to decrease residence time of the fuel between the nozzle and the measuring position. This reduction of the residence time will materially reduce the fuel vaporized and appears to be the most important factor under this set of conditions.

CONCLUSIONS AND RECOMMENDATIONS

As a result of these tests is is concluded that:

1. The results obtained during these tests are qualitatively correct.
2. The spray characteristics are important in the range of conditions investigated during these tests.
3. Under the conditions of these tests, the parameters investigated have the following effect on the vaporization of the spray:
    a. Increasing air temperature, increases the fraction vaporized.
    b. Increasing pressure decreases the fraction vaporized.
    c. Increasing velocity decreases the fraction vaporized.
    d. Increasing fuel-air ratio first decreases then increases the fraction vaporized.
4. The performance of the basic equipment is not satisfactory to conduct fuel vaporization studies. The prime shortcoming being the large temperature gradient in the test section.
5. The thermocouple configurations used during these tests, to measure the mixture temperature, do not give correct readings. It is further concluded that the two configurations have merit and that minor modification should greatly improve the accuracy of the measurements.

As a result of these tests it is recommended that:

1. No further fuel vaporization test be attempted until the test section temperature gradient is eliminated. Possible solutions to this problem include; placing the tunnel in a vertical position; increasing the overall range of operation of the tunnel, thereby, increasing the velocities in the settling chamber; very closely investigating and eliminating heat loss through the walls; and the use of variable porosity screens in the tunnel.
2. The fuel system capacity be increased by use of a larger nozzle and the cone angle of the spray be decreased to prevent impingement on the walls so near the injection point.
3. The thermocouple configurations (b) and (c) of Fig. 7, be redesigned to reduce conduction losses.
4. The redesign of configuration (c) of Fig. 7 include an ogival nose in place of the flat plate to insure flow of air from the back of the probe over the element and out through the space at the junction of the nose and main body.
5. The tunnel be moved from its present location to a room away from the engine and compressor to improve the habitability in the vicinity of the tunnel and also to eliminate the effect of the air currents present in the engine room.
6. Only a minimum of time be spent trying to correct the defects of this equipment. If rapid progress is not indicated, discard this piece of equipment.

APPENDIX

Development of Operating Curves

To facilitate the operation and control of the tunnel, a number of operating curves were developed. These curves were to simplify the determination of control values for different values of the primary variable during a run.

$$P_{dy} = \frac{\rho}{2} V^2$$

or but $\rho = \frac{P}{RT}$

$$V_a = \sqrt{\frac{2 P_{dy}}{\rho}}$$

$$V_a = \sqrt{\frac{2 P_{dy} R T_{ts}}{P_{ts}}} = 58.57 \sqrt{\frac{P_{dy} T_{ts}}{P_{ts}}}$$

V is the air velocity in the test section (ft/sec), where P_{dy} is the test section dynamic pressure (lb/ft^2), P_{ts} is the test section absolute pressure (lb/ft^2) and T_{ts} is the test section temperature (^oR). Now convert to units actually used in the control of the tunnel, change P_{dy} from lb/ft^2 to inches alcohol inclined at 30^o and P_{ts} to inches mercury, absolute. Solve for $(P_{dy})_{al}$;

$$(P_{dy})_{al} = \frac{V_a^2 (P_{ts})_h}{101.8 T_{ts}}$$

For the mass flow rate of the air:

$$\dot{m}a = \rho_a A_{ts} V_a$$

or substituting the above expression for V_a:

$$\dot{m}_a = 1.48\sqrt{\frac{(P_{dy})_{al}\,(P_{ts})_h}{T_{ts}}} = .147\,\frac{V_a(P_{ts})_h}{T_{ts}}$$

Now $\dot{m}_f = F\dot{m}_a$, converting this to gal/hr gage reading,

$$(\dot{m}_f)_g = 675\,F\dot{m}_a = (99.1)F\,\frac{V_a(P_{ts})_h}{T_{ts}}$$

These equations can then be plotted in any manner desired, for instance, $(P_{dy})_{al}$ versus T_{ts} at a constant velocity and pressure.

Estimation of Thermocouple Error

To estimate the thermocouple error, the thermocouple temperature was calculated for a typical value of air temperature in the test section. These calculations are for configuration (b) of Fig. 7. The calculations were made in two parts; first, consider the supporting tube to be a fin projecting from the wall and calculate the temperature at the end supporting the thermocouple junction; second, consider the thermocouple to be a fin projecting from the end of the supporting tube and calculate the temperature at the free end. This then is the calculated thermocouple temperature. The difference between the assumed air temperature and the calculated thermocouple temperature is the thermocouple error. This error being correct to the validity of the calculations and assumptions.

The following equation applies:

$$t_t - t_a = \frac{t_m - t_a}{\text{Cosh } Ml} \qquad \text{where} \qquad M = \sqrt{\frac{hC}{kA}}$$

Apply this equation first to the supporting tube, using the following values and equations to evaluate the terms of the original equation.

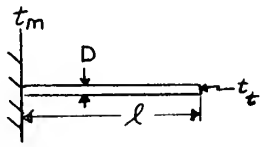

l = 0.166 ft.

tube OD = 0.082 in.

tube ID = 0.060 in.

k = 25 BTU/ft^2-hr-^{o}F/ft.

t_m = 180^{o}F

t_a = 220^{o}F

$$A = \frac{\pi}{(4)144}\left[(OD)^2-(ID)^2\right] = 0.0000171 \text{ ft}^2$$

$$C = \frac{\pi \text{ OD}}{12} = 0.0214 \text{ ft.}$$

Taken from page 115 of Ref. 11 is the following equation for air:

$$\frac{hD}{k} = 0.3\left[\frac{VD\rho}{\mu}\right]^{0.57}$$

where h is the surface film heat transfer coefficient (BTU/ft^2-hr-^{o}F), D is the tube diameter (ft), k is the thermal conductivity of air (BTU/ft^2-hr-^{o}F/ft), V is the air velocity (ft/hr), ρ is the air density (lb /ft^3) and μ is the absolute visosity of the air (lb/ft-hr). This equation applies to single tubes and wires in air, normal to the flow. Solving this for h,

$$h = 0.3\,\frac{k}{D}\left[\frac{VD\rho}{\mu}\right]^{0.57}$$

Now substituting:

$k_a = 0.0182$ BTU/ft^2-hr-$^\circ$F/ft.

$D = \frac{.082}{12}$ ft.

$V = 70$ ft/sec.

$\rho = .0584$ lb/ft^3

$\mu = .0532$ lb/ft-hr.

Then:

$h = 58.2$ BTU/ft^2-hr-$^\circ$F.

And:

$M = \sqrt{2910} = 54.0$ 1/ft.; $Ml = \frac{54.0}{6} = 9.0$

Cosh Ml = 4051.0

Finally:

$$t_t = \frac{t_m - t_a}{\text{Cosh Ml}} + t_a = \frac{180 - 220}{4051.0} + 220$$

$= 220.0^\circ$F.

Thus the temperature of the free end of the supporting tube when the wall is assumed to be at 180°F and the air temperature is assumed 220°F is very nearly the assumed air temperature. This then becomes effectively the temperature of the wall when considering the thermocouple junction.

Apply the same equations to the thermocouple junction, with appropriate values, and consider now also the radiation losses. For the thermocouple element the following values are used:

$l = \frac{1}{2}$ in. $= 1/24$ ft.

D = twice the diameter of one wire.

$= \frac{0.02}{12}$ ft.

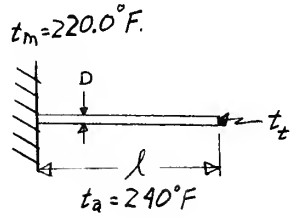

C = twice the circumference of one wire (# 30 Wire)

$= \frac{2\pi\ (.01)}{12} = 0.00523$ ft.

A = twice the area of one wire.

$= (2) \left[\frac{\pi(.01)^2}{4(144)}\right] = .00000109\ ft^2$

$k = \frac{k_{iron} + k_{constantan}}{2} = \frac{36+15}{2} = 25$ BTU/hr-ft^2-^oF/ft

Now considering and combining the effects of convection and radiation:

$h = h_{cv} - h_r$

$h_{cv} = (0.3) \frac{K}{D} \left[\frac{VD\rho}{\mu}\right]^{0.57}$

$h_r = \frac{\sigma\epsilon(T_t^4 - T_s^4)}{T_t - T_a}$ (Considering for h_r that the element radiates only to the shield)

where h_r is the radiation heat transfer coefficient (BTU/ft^2-hr-^oF), σ is the Stefan-Botlzmann constant (BTU/hr-ft^2-T^4), T_t is the thermocouple temperature (^oR), T_s is the shield temperature (^oR), T_a is the air temperature (^oR) and ϵ is the emmissivity.

Now continuing with values to be substituted:

$D = \frac{.02}{12}$ ft.

V = 10 ft/ sec., since the element is located behind the shield.

$\rho = .0568$ lb /ft^3

$\mu = .0543$ lb/ft-hr.

$k_a = .0186$ BTU/ft^2-hr-^oF/ft.

$\sigma = 0.1728 \times 10^{-8}$ BTU/hr-ft^{2}T^4

$\epsilon = 0.9$

$T_t = 700^{\circ}R.$

$T_s = 660^{\circ}R.$

Substitution of these values gives:

$h_{cv} = 35.5$ BTU/hr-ft^2-$^{\circ}$F.

$h_r = 15.6$ BTU/hr-ft^2-$^{\circ}$F.

or adding

$h = h_{cv} - h_r = 19.9$ BTU/hr-ft^2-$^{\circ}$F.

and

$M = 61.3$ 1/ft.

$Ml = 2.56$

Cosh $Ml = 6.5$

and finally

$$t_t - t_a = \frac{t_m - t_a}{\text{Cosh } Ml} = \frac{220 - 240}{6.5} = -3.08^{\circ}F.$$

This is then the thermocouple error as calculated by the foregoing method, assumptions and values.

The value of the error is very sensitive to the velocity over the element and to the length of immersion. The effect of the velocity being felt through its effect on h. The effect of the length of immersion is felt through its effect on Ml and Cosh Ml. The length of immersion effects the error directly since Cosh Ml is divided into the difference of the wall and air temperature to give the error, i.e. the difference between the air and thermocouple temperature. The value calculated appears to be very much too low, evidently other errors not taken into consideration in this calculation are important and have appreciable effect on the results.

Calculation of Maximum Temperature Drop

$$(\Delta T)_{max} = \frac{FH_v}{c_{p_a}+Fc_{p_f}} + \frac{Fc_{pf}}{c_{p_a}+Fc_{p_f}} (T_{a_I} - T_{f_I})$$

This assumes that the fuel has just completely vaporized.

Substituting the following numerical values:

$F = 0.01925$

$c_{p_a} = .24$ BTU/lb-^oF

$c_{p_f} = .42$ BTU/lb-^oF

$H_v = 170$ BTU/#

$T_{a_I} = 700^oR$

$T_{f_I} = 518^oR$

gives the following:

$\Delta T = 13.2 + 5.95$

$= 19.15^oF.$

Calculation of Fuel Exit Velocity

$D_0 = 0.0215$ in.

$A_0 = 0.000364$ in^2.

$\dot{m}_f = \rho_f A_0 V_f$

fuel density = 62.4 x 0.877 = 54.5 lb/ft^3

$$V_f = \frac{\dot{m}f}{\rho_f A_0}$$

Converting to units of gal/hr, gage.

$V_f = 10.78(\dot{m}_f)_g$

or for $F = .01925$, $V_a = 70$ ft/sec, $t_a = 240^oF$, and $(P_{ts})_h = 26$ in. hg., absolute

$V_f = 52.82$ ft/sec.

REFERENCES

1. Ingebo, Robert D., "Vaporization Rates and Heat-Transfer Coefficients for Pure Liquid Drops." National Advisory Committee for Aeronautics, Technical Note 2368, July, 1951.

2. Ingebo, Robert D., "Study of Pressure Effects on Vaporization Rate of Drops in Gas Streams." National Advisory Committee for Aeronautics, Technical Note 2850, January, 1953.

3. El-Wakil, M.M., Uyehara, O.A., and Meyers, P.S., "A Theoretical Investigation of the Heating-Up Period of Injected Fuel Droplets Vaporizing in Air." National Advisory Committee for Aeronautics, Technical Note 3179, May, 1954.

4. El-Wakil, M.M., Priem, R.J., Brikowski, H.J., Meyers, P.S., and Uyehara, O.A., "Experimental and Calculated Temperature and Mass Histories of Vaporizing Fuel Drop." National Advisory Committee for Aeronautics, Technical Note 3490, January, 1956.

5. Foster, Hampton H. and Ingebo, Robert D., "Evaporation of JP-5 Fuel Sprays in Air Streams". National Advisory Committee for Aeronautics Research Memorandum E55K02.

6. Bahr, Donald W., "Evaporation and Spreading of Iso-Octane Sprays in High-Velocity Air Streams." National Advisory Committee for Aeronautics, Research Memorandum E53114.

7. Ingebo, Robert D., "Vaporation Rates and Drag Coefficients for Iso-Octane Sprays in Turbulent Air Streams." National Advisory Committee for Aeronautics, Technical Note 3265.

8. Bailey, John B., "Preliminary Testing of an Experimental Apparatus Designed for Study of Fuel Spray Vaporization in Jet Engine Combusters." A Master of Science Thesis submitted to the University of Minnesota, 1955.

9. Farnsworth, William D., "The Design of a Wind Tunnel for fuel Spray Vaporization Studies." A Master of Science Thesis submitted to the University of Minnesota, 1955.

10. Brown, Aubrey I. and Marco, Salvatore M., "Introduction to Heat Transfer." First Edition Seventh Impression. New York, McGraw-Hill Book Company, Inc., 1942.

11. Jakob, Max, and Hawkins, George A., "Elements of Heat Transfer and Insulation." Second Edition, New York, John Wiley and Sons, Inc.

12. Carlson, Walter O., "Interferometric Studies of Connective Flow Phenomena in Vertical, Plane Enclosed Air Layers. A Doctor of Philosophy Thesis submitted to the University of Minnesota, 1956.

Test No. IV Date 24 April Constants V = 70 fps, P_{ts} = 24 "Hg, F = .01925 Time began 1400 Time ended 1620

Variable T

Run #	V	P_{ts}	t_{ts}	F/A	Cond	P_{dy_2}	P_{ts}	t_1	t_9	t_9'	t_{10}	$\dot{m}_f$	t_{ab}	Heat. Pat.	RPM	Bleed	
	ft/sec	in.Hg. abs.	°F			in. alc 30°	in.Hg. vac.	°F	°F	°F	°F	gph gage	°F				
I	70	24	–	.01925	dry	1.8	5.45	180	185	187	182	5.0	74	⌐	1920	open	
					wet	1.8	5.45	183	160	114	165						
							-ΔT	-3	25	73	17						
II	70	24	–	.01925	dry	1.7	5.43	225	216	216	210	4.7	74	⌐	1920	open	
					wet	1.7	5.43	228	178	144	190						
							-ΔT	-3	38	72	20						
III	70	24	–	.01925	dry	1.62	5.45	265	260	260	251	4.9	72	⌐	1920	open	
					wet	1.62	5.45	267	215	184	233						
							-ΔT	-2	45	76	24						
IV	70	24	–	.01925	dry	1.55	5.44	300	323	323	325	4.2	70	⌐	1920	open	Use t_1 as 312.5°
					wet	1.55	5.44	302	268	237	291						
							-ΔT	-2	55	86	34						

Run # I

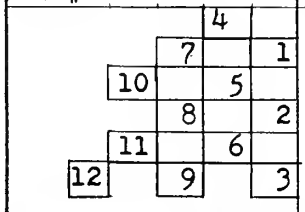

Run # II

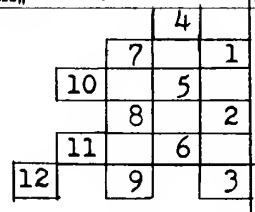

Run # III

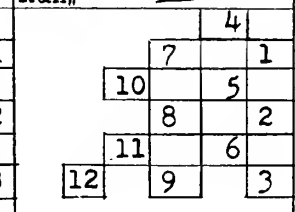

Run # IV

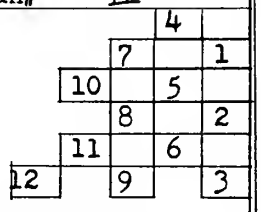

t_f 58° F
$t_{w_{in}}$ 58°F
$t_{w_{out}}$ 58°F
$P_{bar.}$ 29.46 "Hg

Posit. in.	top	0.5	1.0	1.5	2.0	2.5	3.0	3.5	bot.
t_1 °F	–	410	350	300	290	290	288	–	–

Taken after Run # IV
$t_{1(avg)}$ = 312.5° F

TABLE I.- Sample data sheet and typical data.

TABLE II

PROPERTIES OF TECHNICAL BENZOL (BENZENE)

Chemical formula	$C_6 H_6$
Molecular weight	78.11
Hydrogen carbon ratio	.0835
Boiling point of liquid, °F	176.2
Density at 65°F lb/gallon liquid	7.31
Specific gravity at 65°F	.877
Latent heat of vaporation BTU/lb	
68°F	187
104°F	181
176°F	170
Oxygen required for combustion, per lb	3.1
Air required for combustion, per lb	13.32
Fuel-air ratio for combustion, per lb	.075
Lower Heating value, BTU/lb	17259
Mean specific heat at 1 atm, 93°F to 240°F	.42
Specific heat ratio, 1 atm, 194°F	1.1

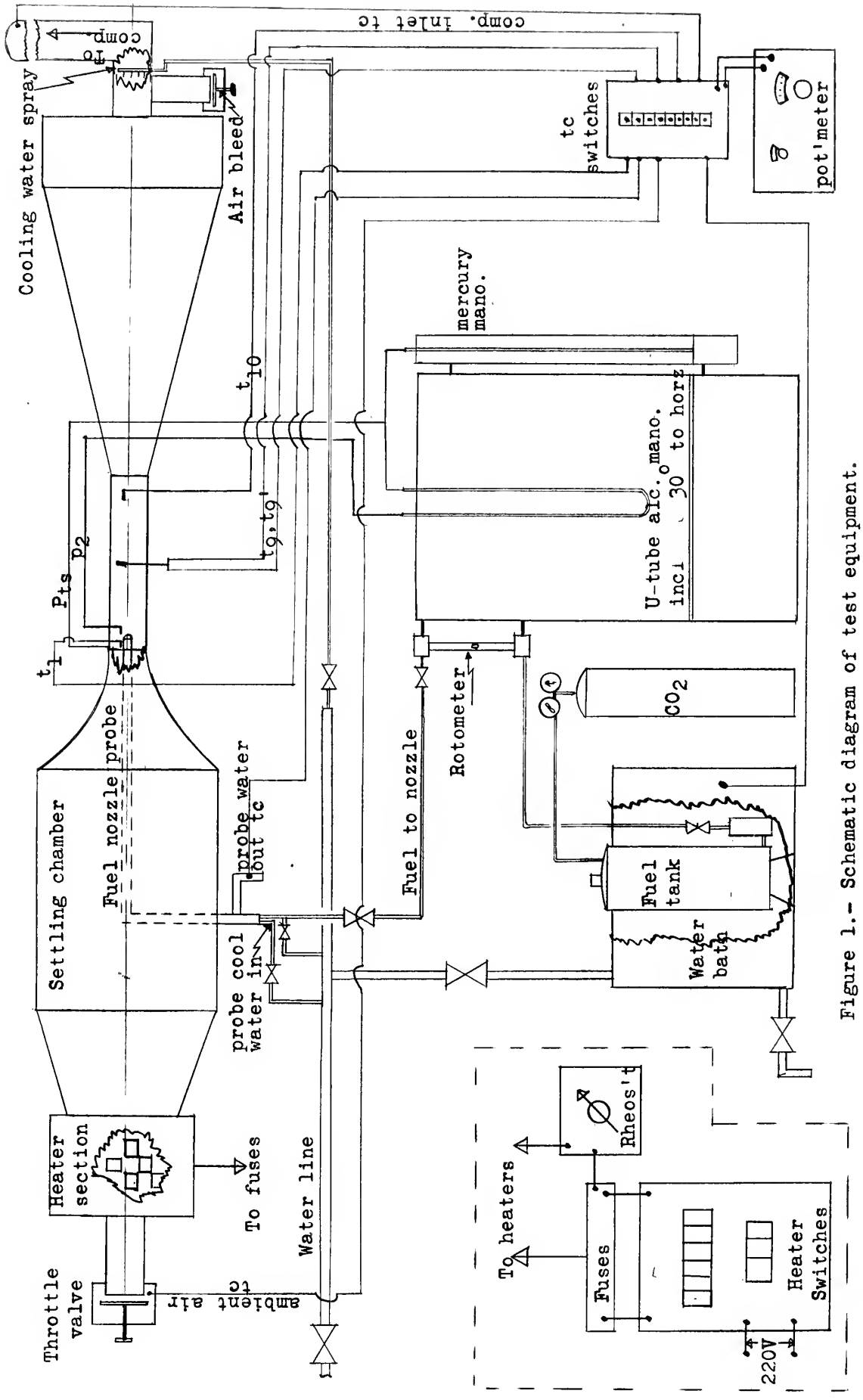

Figure 1.- Schematic diagram of test equipment.

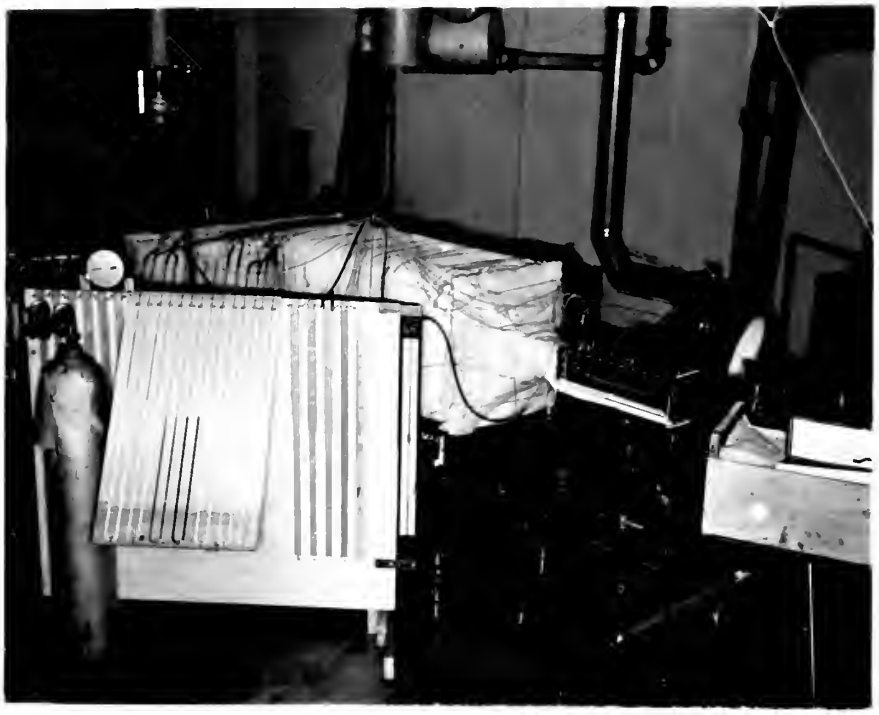

Figure 2. General view of the test equipment.

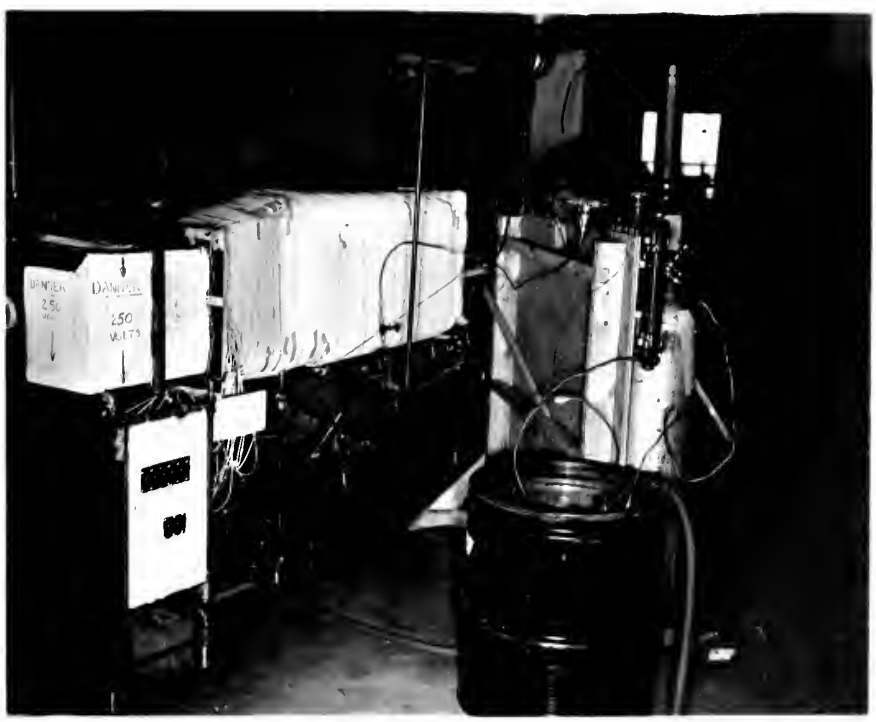

Figure 3. Heater controls and fuel system.

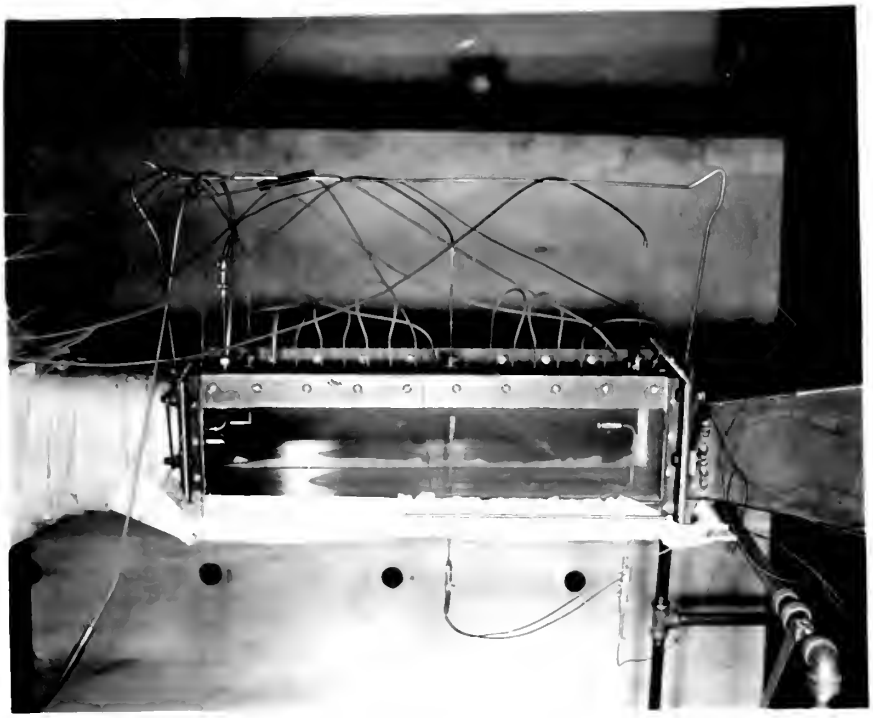

Figure 4. Test section

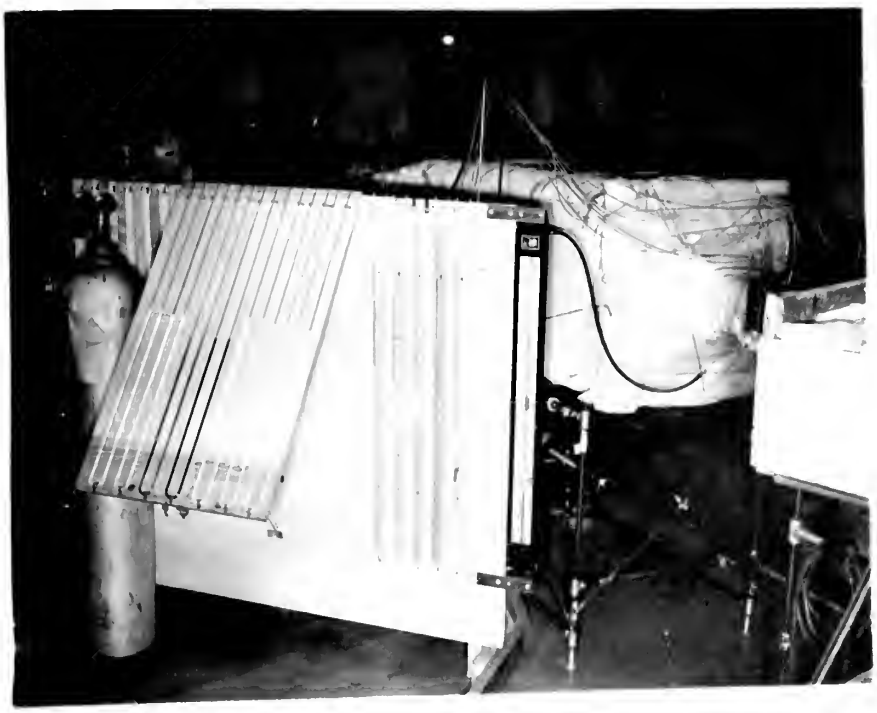

Figure 5. Manometer board

Figure 6. Engine and compressor.

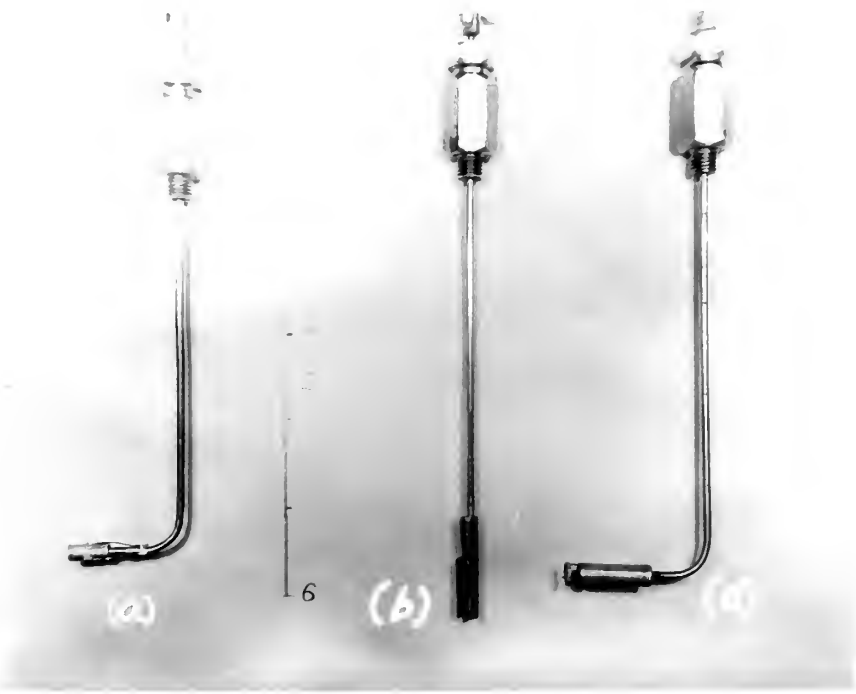

Figure 7. Thermocouple probes.

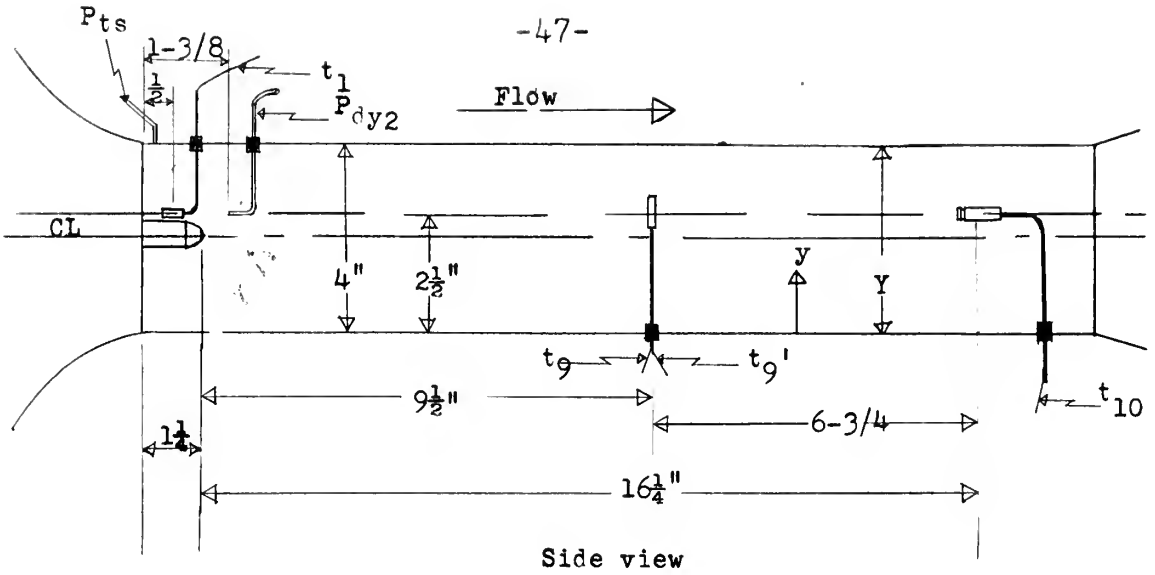

Side view

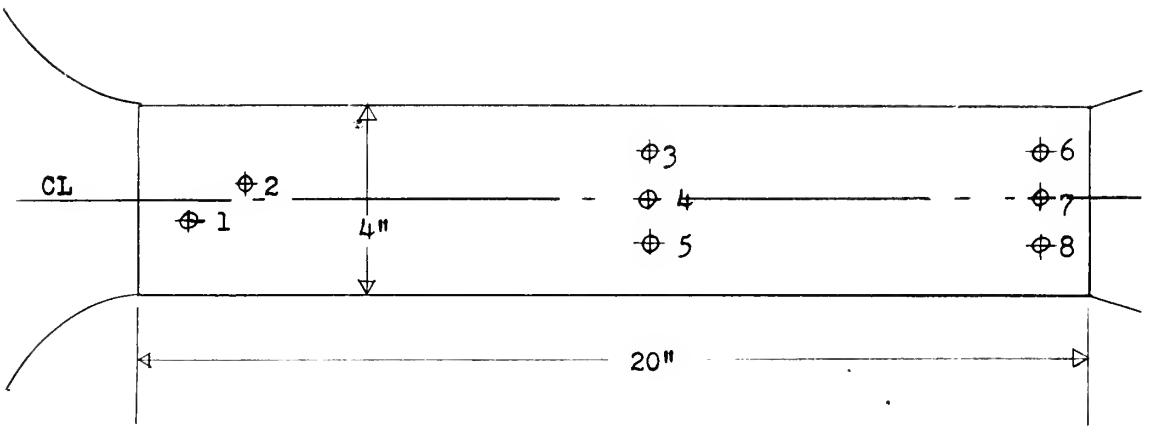

Top view
Numbers in top and bottom view are position numbers

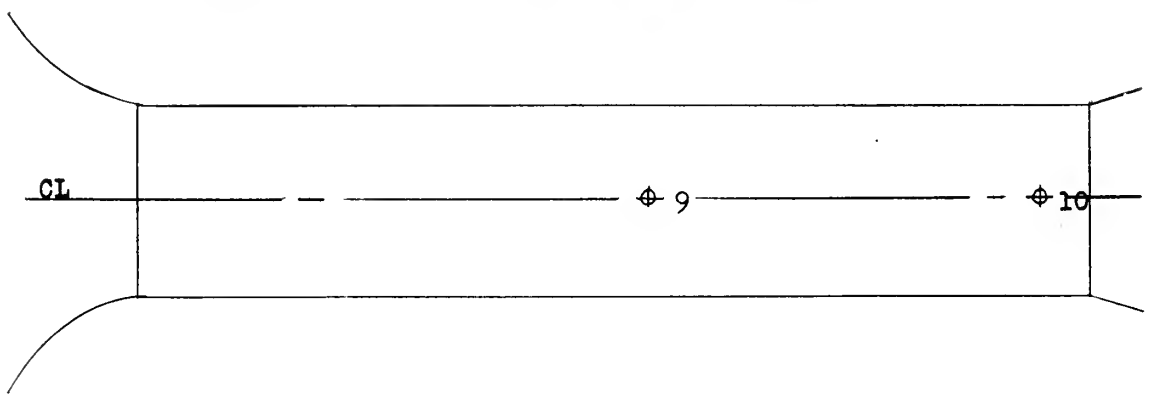

Bottom view

Figure 8. Test section and position numbering

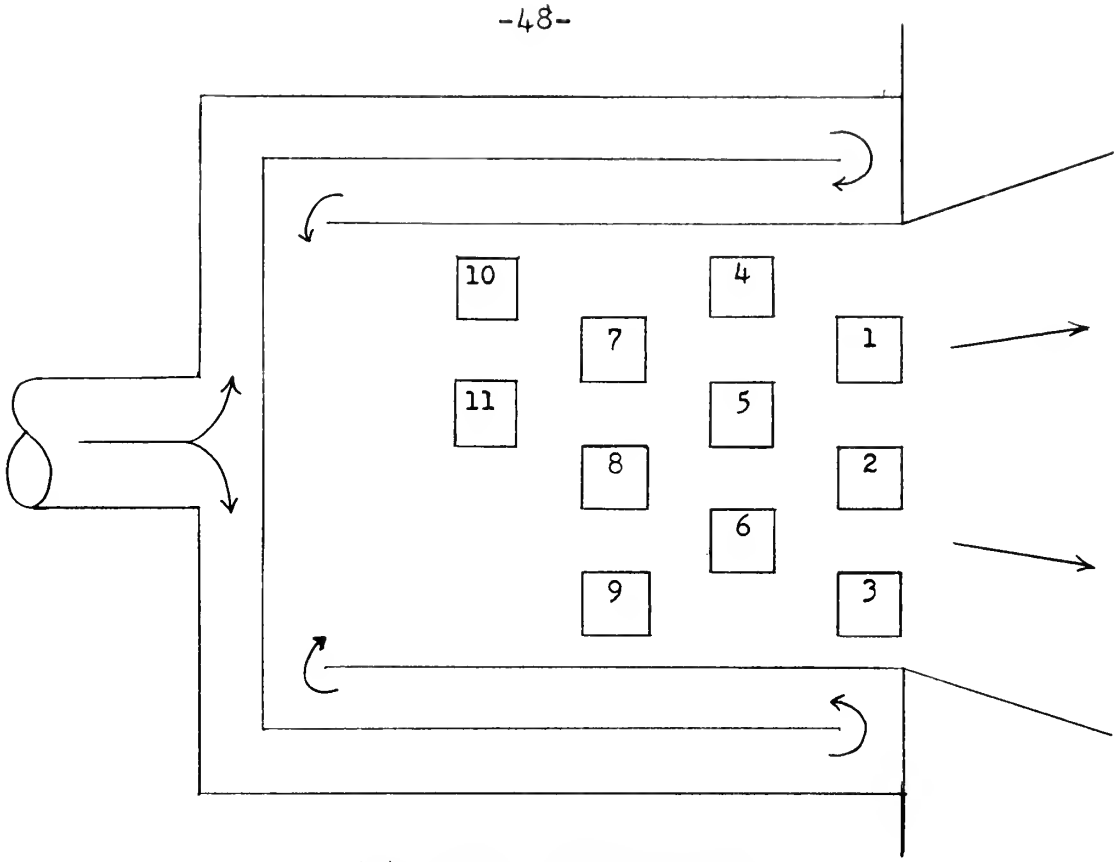

(a) Original Configuration

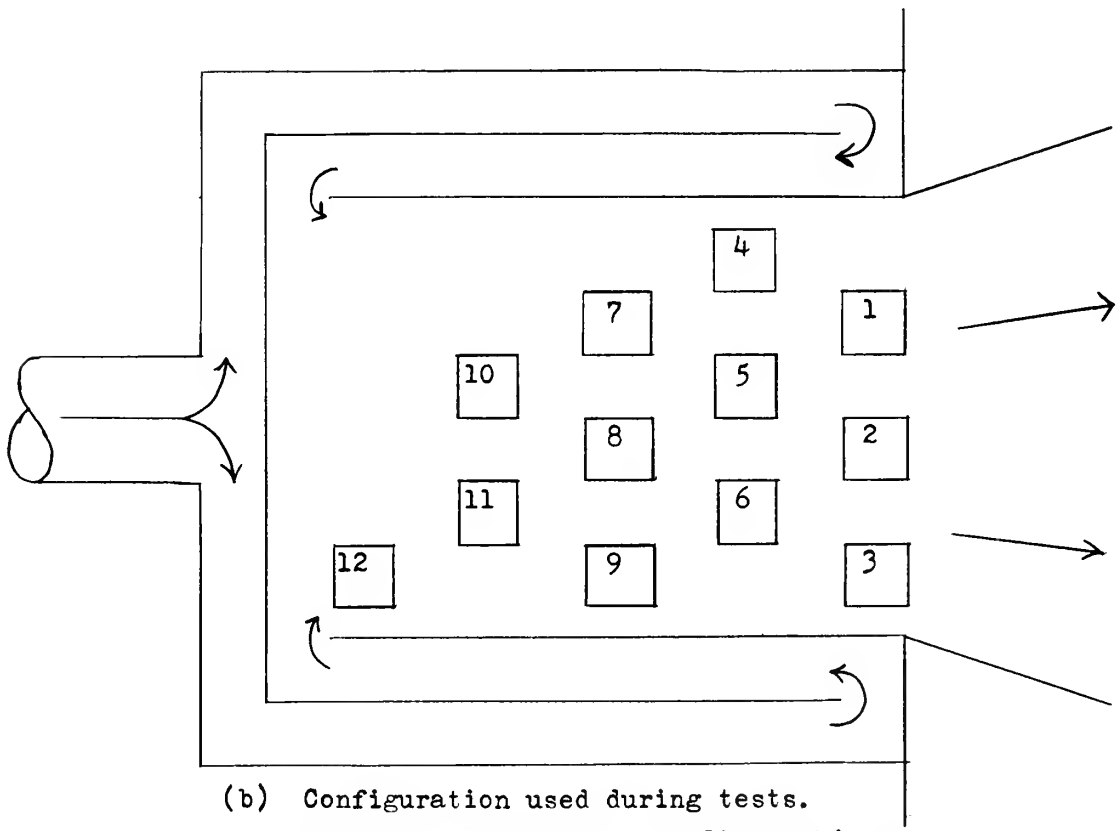

(b) Configuration used during tests.

Figure 9. Heater configurations

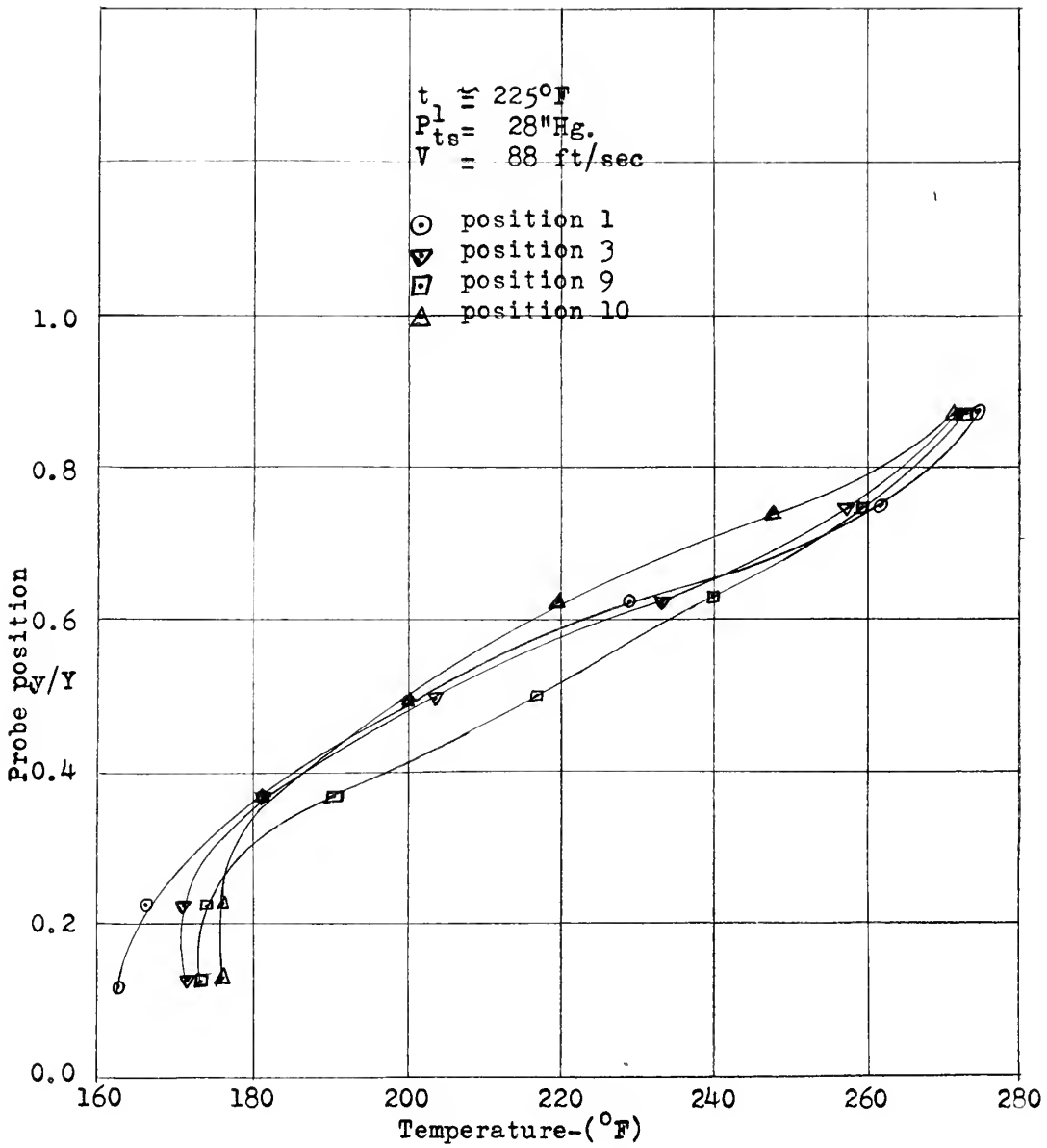

Figure 10. Temperature profiles at various test section positions

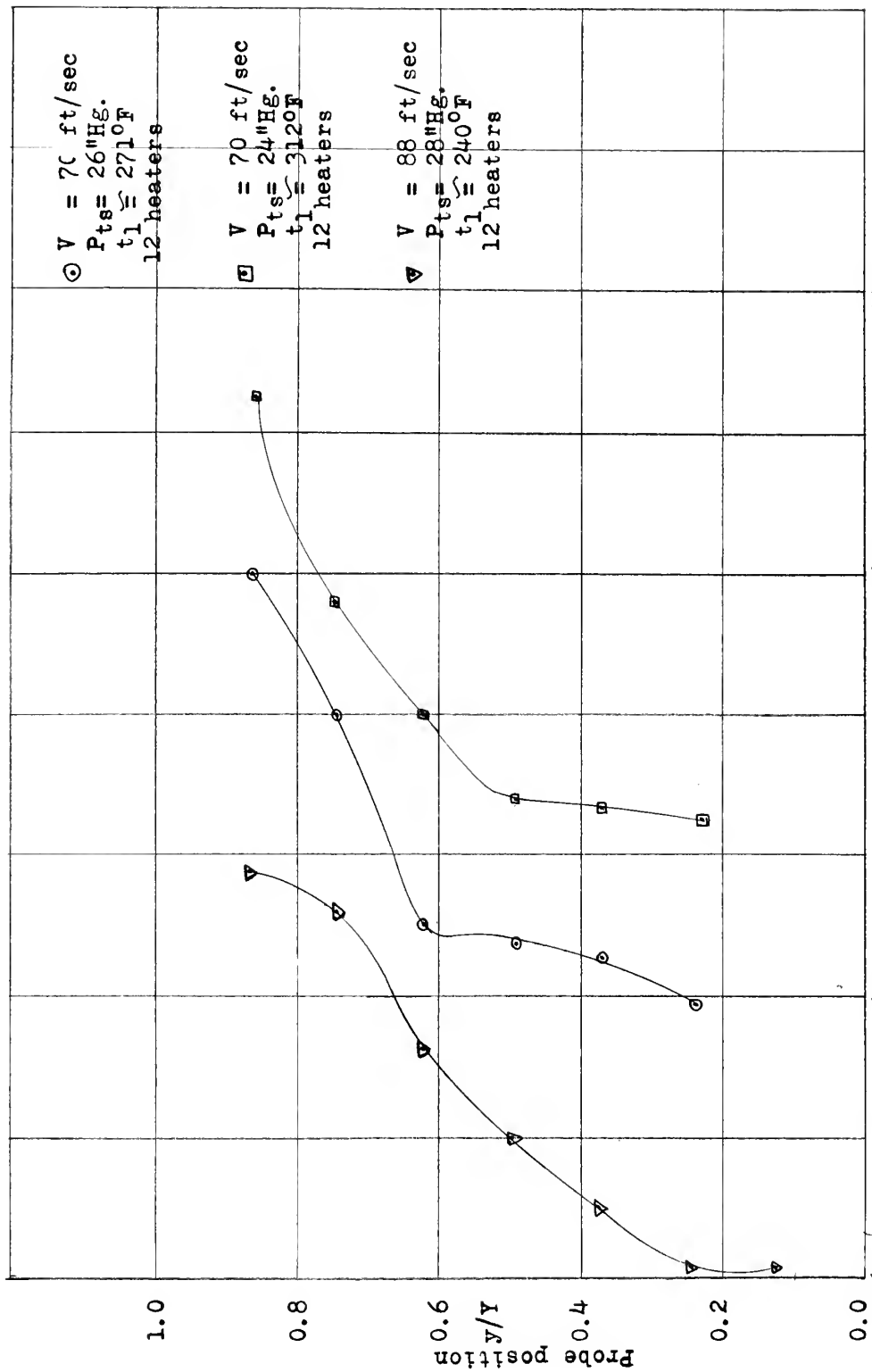

Figure 11.- Temperature profiles at position 1 for various operating conditions.

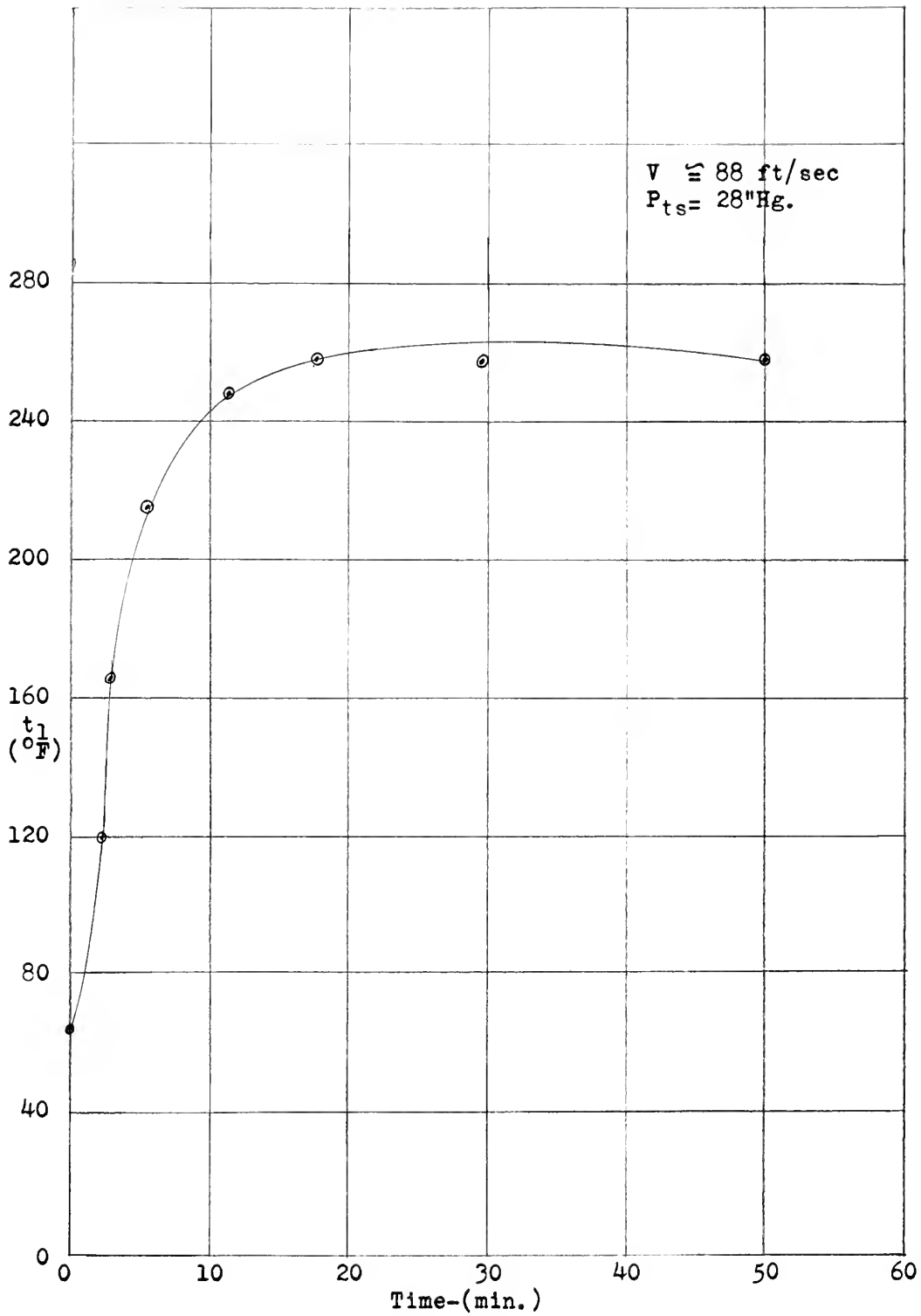

Figure 12. Tunnel heating time

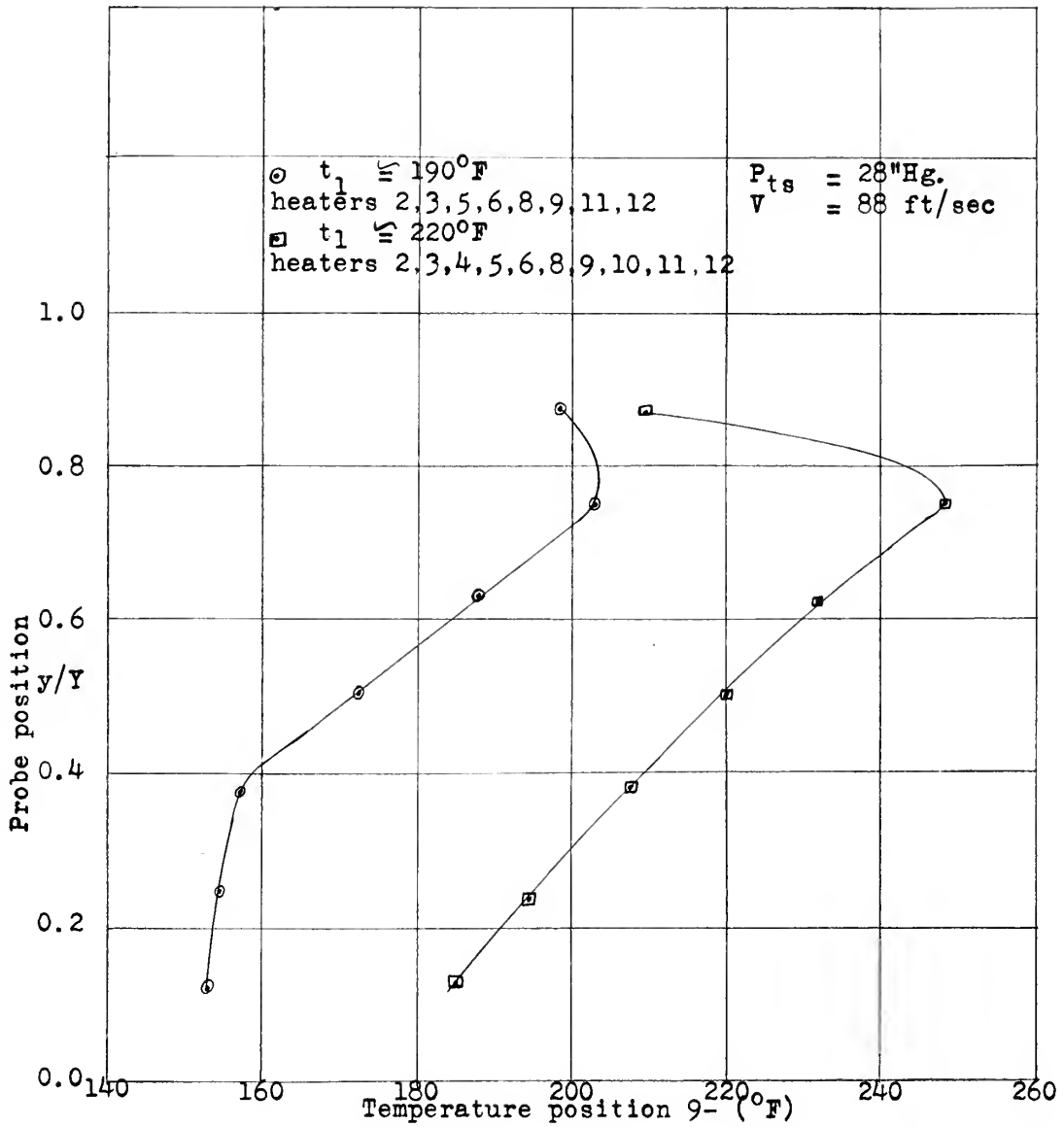

Figure 13. Test section temperature profile with different heaters ON

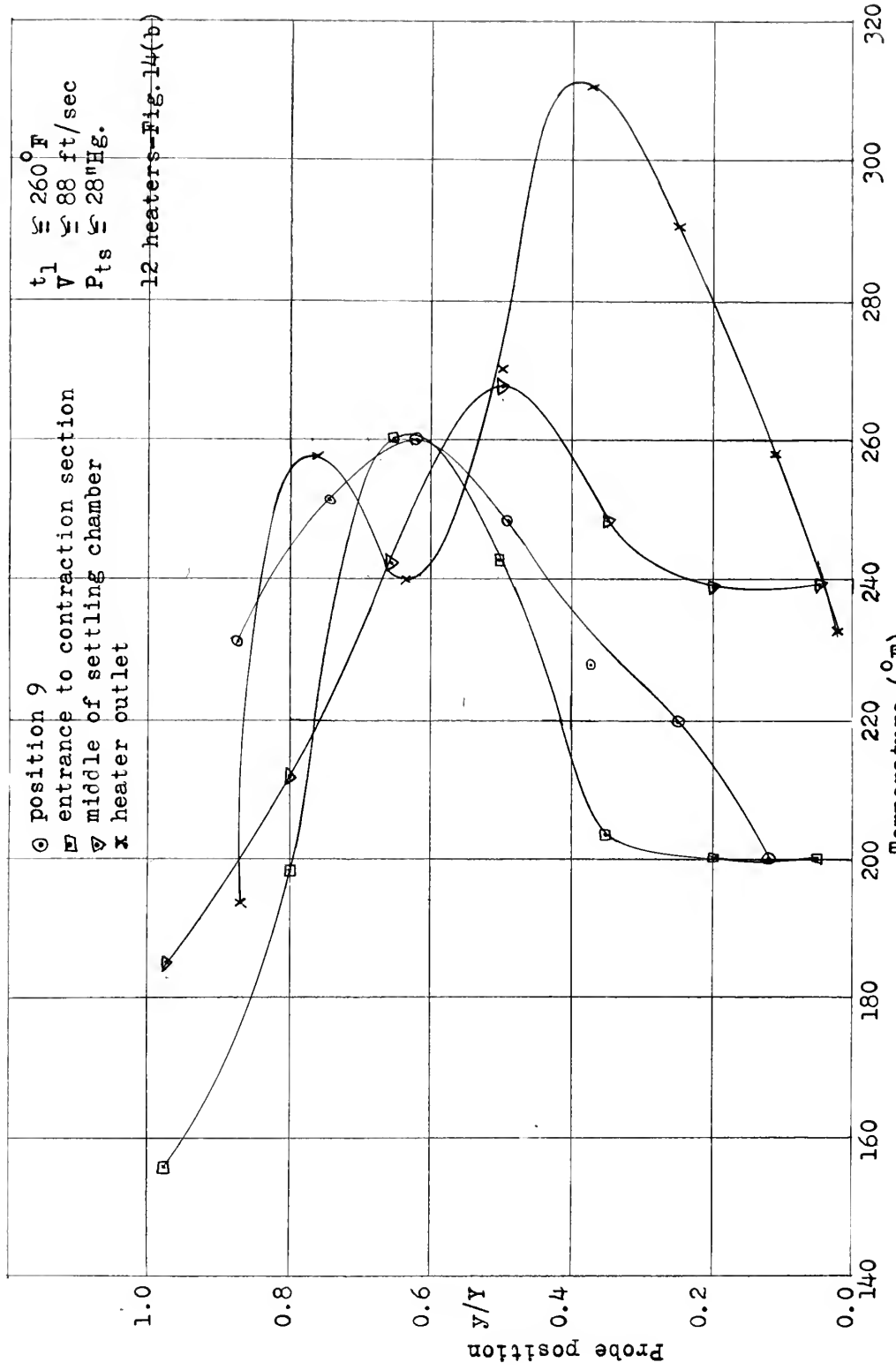

Figure 14.- Temperature profiles at various stations in the tunnel

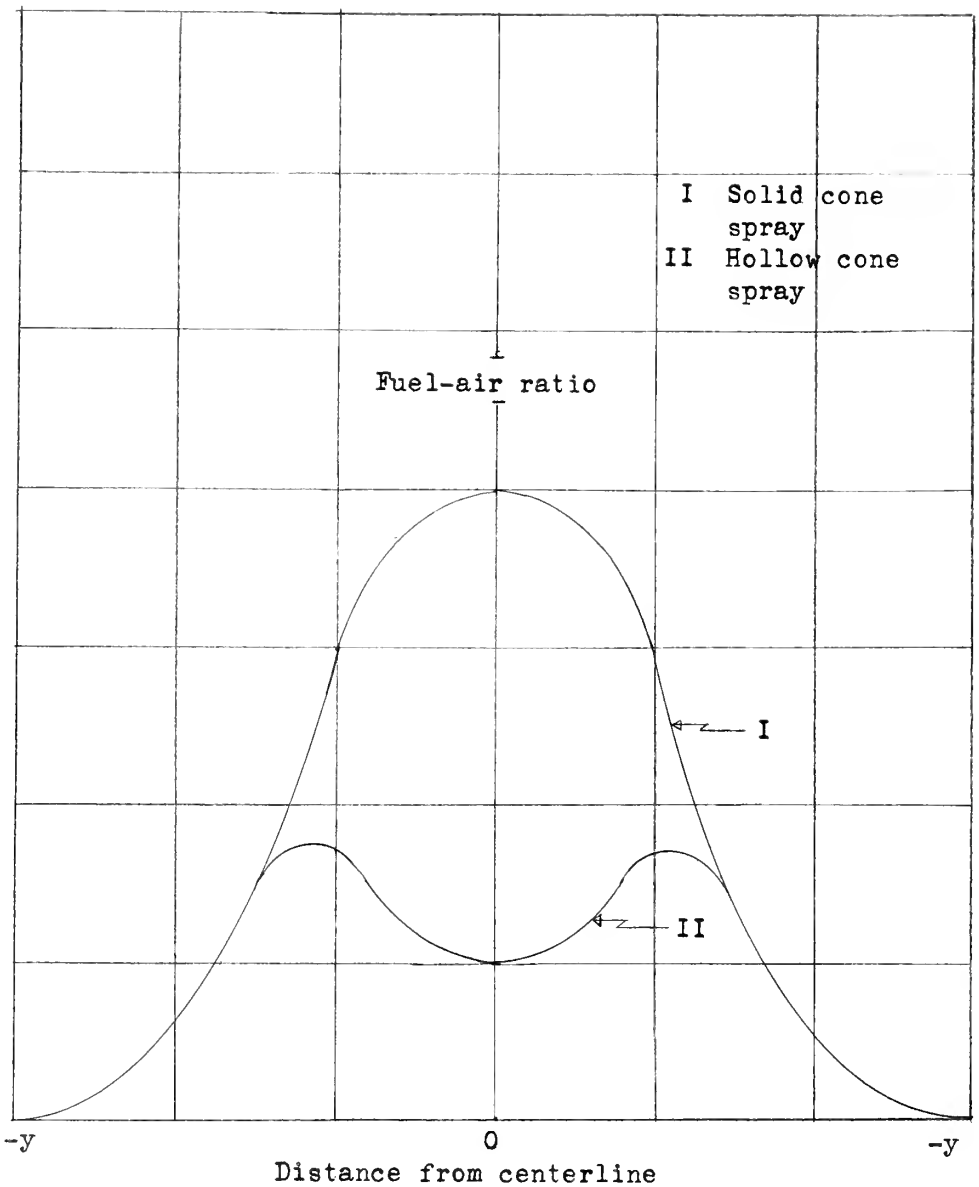

Figure 15. Fuel-air distribution for solid-cone and hollow-cone type spray

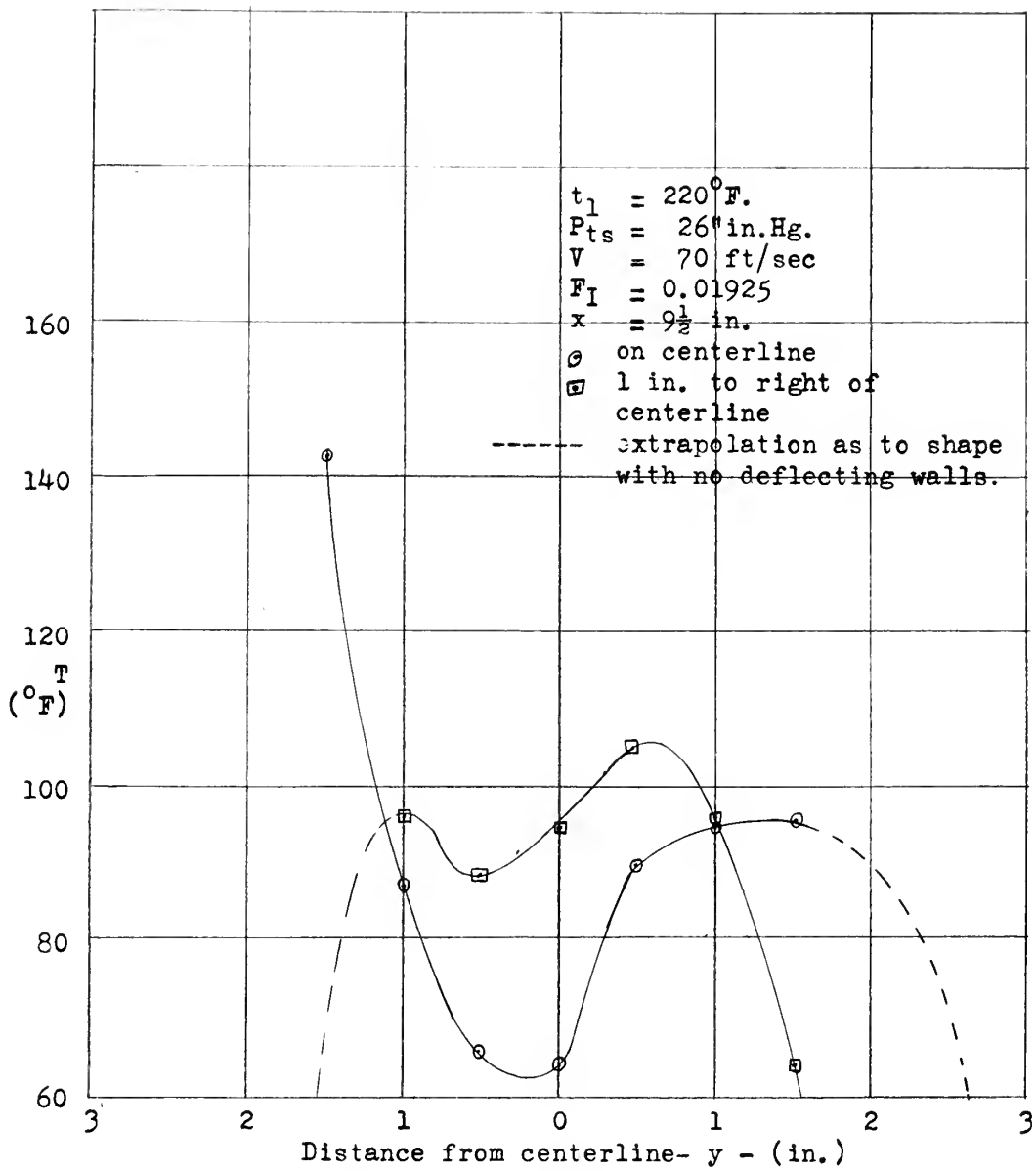

Figure 16. Shield thermocouple temperature drop at various positions in the spray

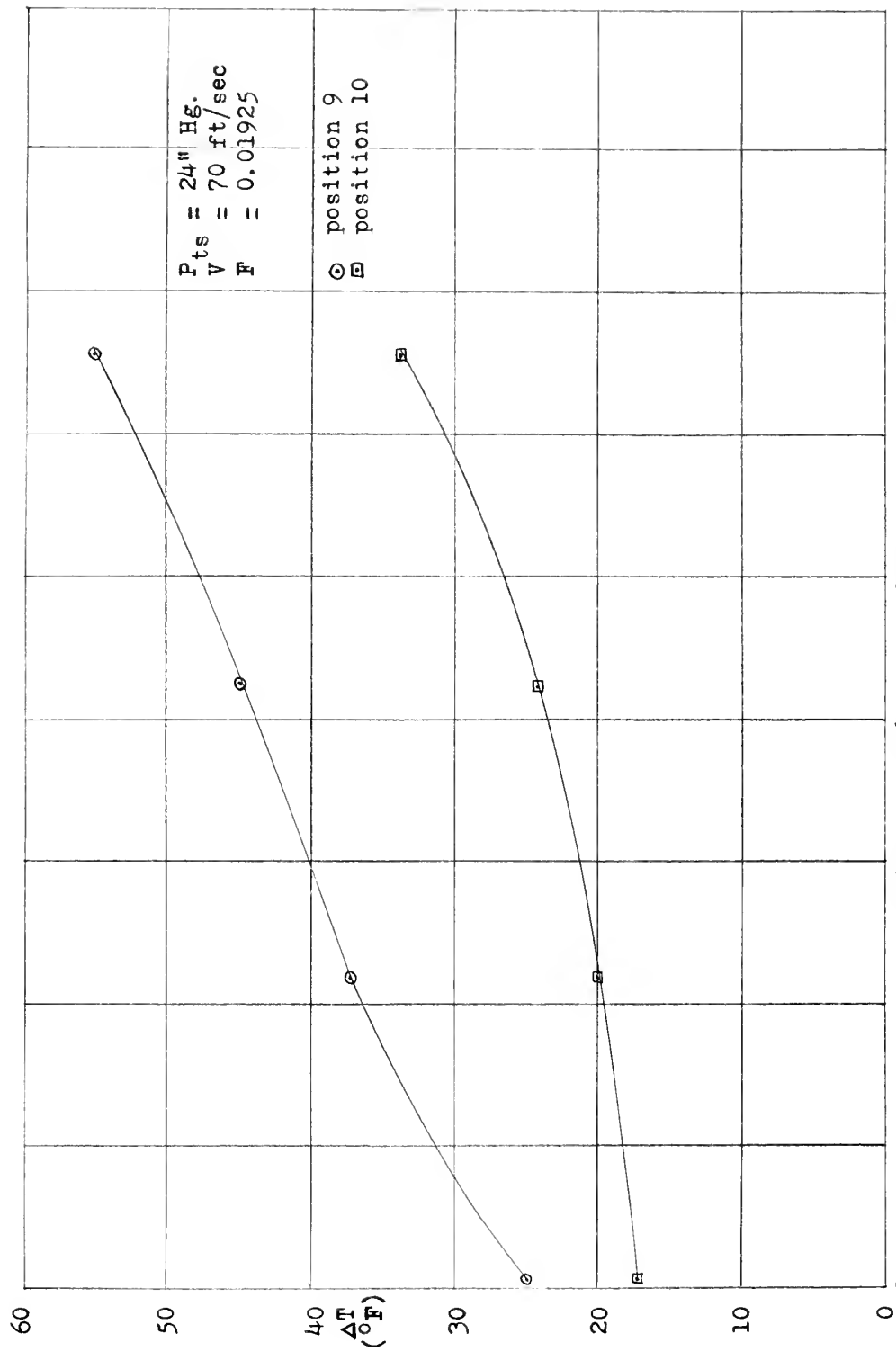

Figure 17.- Effect of air stream temperature on Δ T.

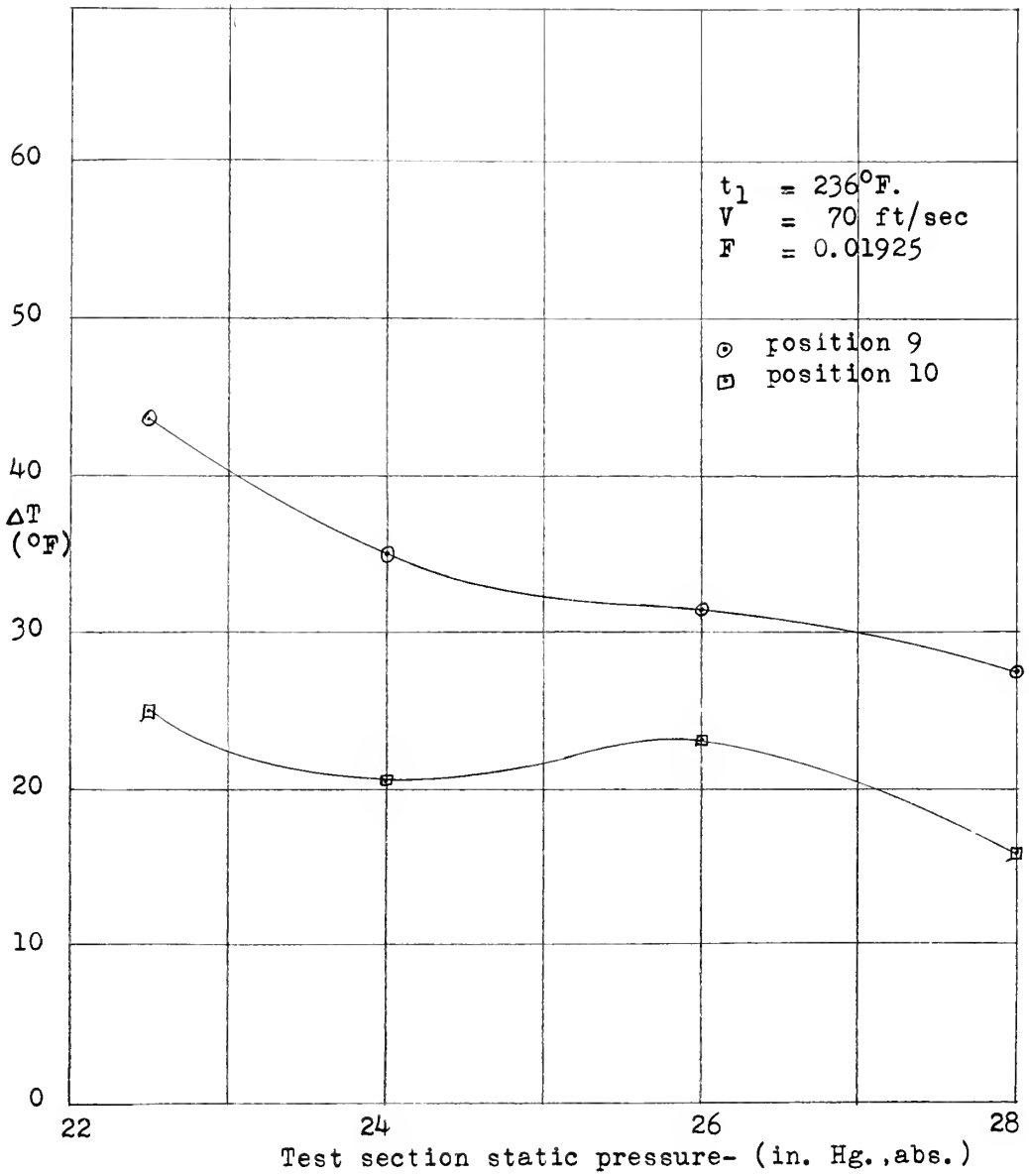

Figure 18. Effect of static pressure on ΔT

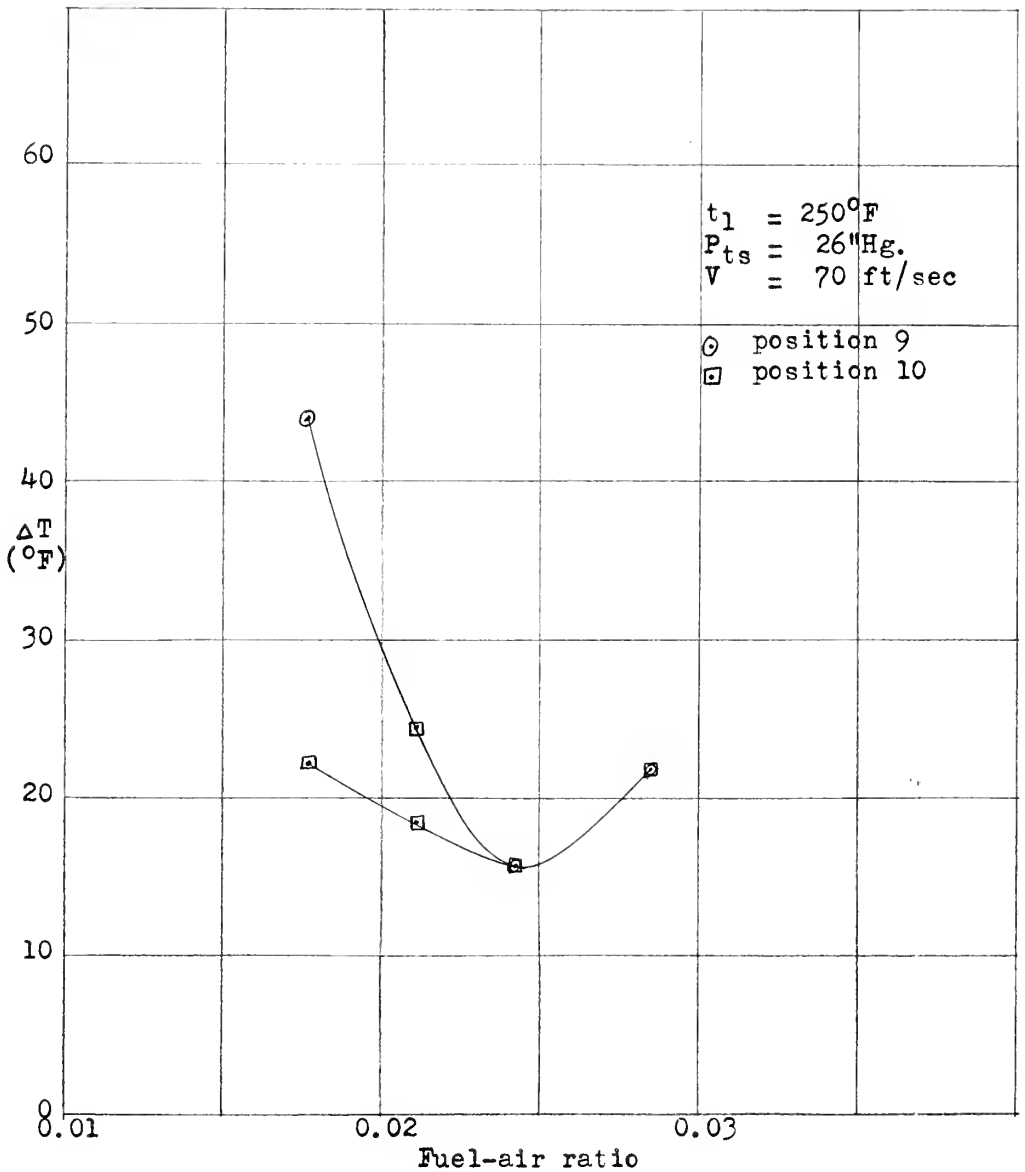

Figure 19. Effect of fuel-air ratio on ΔT

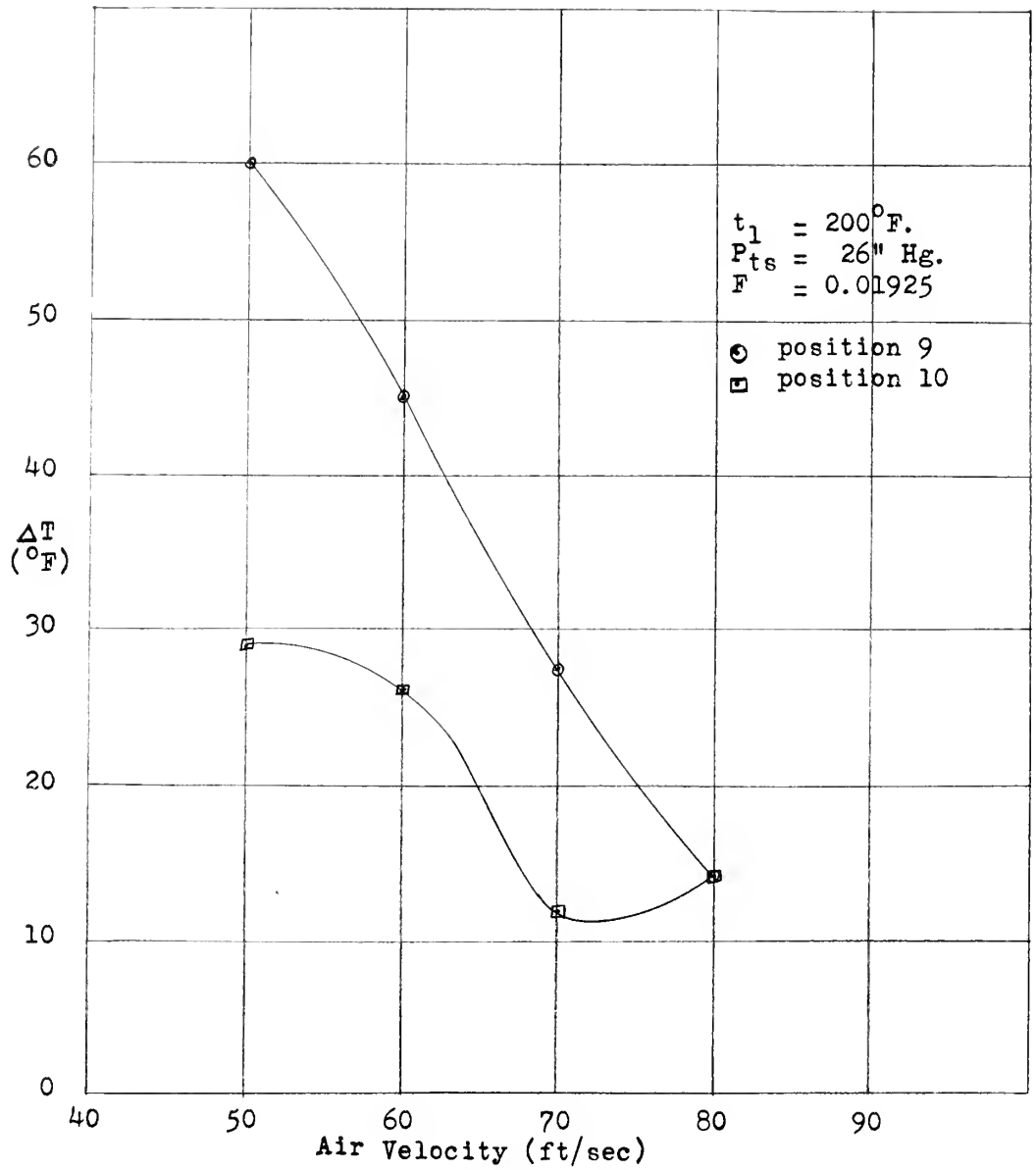

Figure 20. Effect of air stream velocity on Δ T

33165

Thesis
K72 Koch
An investigation of
parameters effecting the
vaporization of fuel...

65

Thesis
K72 Koch
33165
An investigation of parameters
effecting the vaporization of
fuel under conditions
encountered in a turbo-jet
combustion chamber.

thesK72
An investigation of parameters effecting
3 2768 002 11688 1
DUDLEY KNOX LIBRARY